W54w

UNCLASSIFIED

CENTRAL RESEARCH LIBRARY
DOCUMENT COLLECTION

MARTIN MARIETTA ENERGY SYSTEMS LIBRARIES
3 4456 0349671 3

ORNL 1775
Physics

4

SOME IMPROVED MEASUREMENTS OF NUCLEAR MAGNETIC DIPOLE MOMENTS BY MEANS OF NUCLEAR MAGNETIC RESONANCE

H. E. Walchli

CENTRAL RESEARCH LIBRARY
DOCUMENT COLLECTION
LIBRARY LOAN COPY
DO NOT TRANSFER TO ANOTHER PERSON
If you wish someone else to see this document, send in name with document and the library will arrange a loan.

OAK RIDGE NATIONAL LABORATORY
OPERATED BY
CARBIDE AND CARBON CHEMICALS COMPANY
A DIVISION OF UNION CARBIDE AND CARBON CORPORATION
UCC
POST OFFICE BOX P
OAK RIDGE, TENNESSEE

UNCLASSIFIED

UNCLASSIFIED

ORNL 1775

Copy No. 4

SOME IMPROVED MEASUREMENTS OF NUCLEAR MAGNETIC DIPOLE MOMENTS BY MEANS OF NUCLEAR MAGNETIC RESONANCE

Harold E. Walchli

Date Issued

SEP 17 1954

SPECTROSCOPY RESEARCH LABORATORY
J. R. McNally, Jr., Department Head

STABLE ISOTOPE RESEARCH AND PRODUCTION DIVISION
C. P. Keim, Director

OAK RIDGE NATIONAL LABORATORY
Operated by
CARBIDE AND CARBON CHEMICALS COMPANY
A Division of Union Carbide and Carbon Corporation
Oak Ridge, Tennessee

Contract No. W-7405-eng-26

UNCLASSIFIED

MARTIN MARIETTA ENERGY SYSTEMS LIBRARIES

3 4456 0349671 3

INTERNAL DISTRIBUTION

1. C. E. Center
2. Biology Library
3. Health Physics Library
4-5. Central Research Library
6. Reactor Experimental Engineering Library
7-11. Laboratory Records Department
12. Laboratory Records, ORNL R.C.
13. C. E. Larson
14. L. B. Emlet (K-25)
15. J. P. Murray (Y-12)
16. A. M. Weinberg
17. E. H. Taylor
18. E. D. Shipley
19. C. P. Keim
20. W. H. Jordan
21. F. C. VonderLage
22. S. C. Lind
23. F. L. Culler
24. A. H. Snell
25. A. Hollaender
26. M. T. Kelley
27. G. H. Clewett
28. K. Z. Morgan
29. J. H. Frye, Jr.
30. C. E. Normand
31. R. S. Livingston
32. T. A. Lincoln
33. A. S. Livingston
34. C. S. Harrill
35. C. E. Winters
36. D. W. Cardwell
37. E. M. King
38. A. J. Miller
39. D. D. Cowen
40. J. A. Lane
41. Russell Baldock
42. J. R. McNally, Jr.
43. Boyd Weaver
44. P. S. Baker
45. M. J. Skinner
46. S. J. Cromer
47. W. H. Sullivan
48. K. L. Vander Sluis
49. P. M. Griffin
50. H. W. Morgan
51. W. F. Peed
52. S. J. Ovenshine
53-62. H. E. Walchli

EXTERNAL DISTRIBUTION

63. R. F. Bacher, California Institute of Technology
64. Division of Research and Medicine, AEC, ORO
65-317. Given distribution as shown in TID-4500 under Physics category

DISTRIBUTION PAGE TO BE REMOVED IF REPORT IS GIVEN PUBLIC DISTRIBUTION

ABSTRACT

The magnetic moments of nuclei will in general result in a nuclear paramagnetic polarization upon reaching an equilibrium in a constant magnetic field. A high frequency alternating field applied at right angles to the magnetic field will cause a precession of this total polarization about the direction of the steady field, and when the frequency of this alternating field is adjusted to that corresponding with the "Larmor" frequency of the nuclei there will result a component of the polarization at right angles to both of the applied fields. This component of the polarization is used to induce a voltage in a suitably placed coil mounted with its axis collinear with the component.

The design, development, and construction of an instrument, using the method of nuclear induction, and all of its associated magnetic fields and equipment are discussed in detail. This equipment was then used to measure the resonance frequency ratios for 17 isotopes of 13 elements (Li, Na, Al, P, Cl, Cu, Ga, Se, Br, Rb, Cs, Tl) in a fixed magnetic field with a high precision. Twelve of these frequency ratios have not been previously measured and the remaining are in agreement with published values.

ACKNOWLEDGMENT

This report is a portion of a thesis submitted to the University of Tennessee in partial fulfillment of the requirements for a Master of Science in Engineering in June, 1954.

The author is indebted to Dr. E. D. Shipley, Assistant Research Director, ORNL, and to Dr. J. Rand McNally, Jr., of the Spectroscopy Research Laboratory of the Stable Isotope Research and Production Division, under whose direction much of this research has been performed, and to his colleagues in the Laboratory for suggestions and assistance in the construction and operation of portions of the equipment. Appreciation is also expressed to Professor P. C. Cromwell, Dr. F. V. Schultz, and Dr. R. D. Present from the University of Tennessee for their many worthwhile suggestions in the preparation of this report.

TABLE OF CONTENTS

PAGE

INTRODUCTION 1

NOMENCLATURE 3

NUCLEAR RESONANCE THEORY 5

THE NUCLEAR INDUCTION METHOD 14

EQUIPMENT DESIGN 31

The Magnetic System 31

The Frequency Measuring System 43

Frequency Measuring Techniques 45

The Nuclear Induction Spectrometer 49

The Head Unit 49

The Radio-Frequency Amplifier and Detector 54

The Transmitter 57

The Amplifier 57

The Modulating Field 59

THE RESONANCE MEASUREMENTS 62

Lithium 66

Sodium 67

Aluminum 70

Phosphorus 71

Chlorine 71

Vanadium 73

Copper 74

Gallium 76

Selenium 78

PAGE

Bromine 79

Rubidium 81

Cesium 83

Thallium 83

PRECISION OF EXPERIMENTS 85

SUGGESTED IMPROVEMENTS 87

SUMMARY 89

REFERENCES 91

APPENDIX I 97

APPENDIX II 103

APPENDIX III 107

TABLE LIST OF TABLES PAGE

I. Nuclide Frequency Ratio Measurements for Lithium, Sodium, Aluminum, Phosphorus, and Chlorine 68

II. Comparisons of Results for Lithium, Sodium, and Aluminum 69

III. Comparisons of Results for Phosphorus and Chlorine 72

IV. Nuclide Frequency Ratio Measurements for Vanadium, Copper, Gallium, and Selenium 75

V. Comparisons of Results for Copper and Gallium 77

VI. Comparisons of Results for Selenium, Bromine, and Rubidium 80

VII. Nuclide Frequency Ratio Measurements for Bromine, Rubidium, Cesium, and Thallium 82

VIII. Comparisons of Results for Cesium and Thallium 84

LIST OF FIGURES

FIGURES PAGE

1. Classical Mechanical Angular Momentum Relationships 6
2. The Generated Voltage for Rapid Passage 18
3. Schematic of the "Loop" Control 23
4. Single Line Interconnection Diagram of the System 23
5. The Absorption of "v Mode" Resonance Signal 26
6. The Dispersion of "u Mode" Resonance Signal 27
7. Effect of Sample Thickness on Signal Amplitude 30
8. Electromagnet and Coil Detail and Section Drawing 33
9. Electromagnet, Power Supply, and Regulator 34
10. Electromagnet Flux Versus Excitation Current 36
11. Magnetic Field Strength Deviations 37
12. Magnet High Voltage Power Supply Circuit Schematic 39
13. Magnetic Field Regulator Circuit Schematic 40
14. Photograph of Precision Resistor Installed in Regulator . . 41
15. Magnet Field Scanner Control Schematic Diagram 42
16. Assembly Photograph of Nuclear Induction Equipment 50
17. Assembly Detail Drawing for Nuclear Induction Head Unit . . 52
18. Radio-Frequency Amplifier and Detector Schematic 55
19. Transmitter Unit Schematic Diagram 56
20. High-Gain Narrow-Band Amplifier and Phase Detector 58
21. Frequency Characteristics of Narrow-Band Amplifier 60
22. Recorder Control Panel Wiring Schematic 61
23. Phase Shift Oscillator and Modulation Selector 63
24. Variable Frequency Modulating Field Oscillator 64

INTRODUCTION

Many theories have been suggested for the configuration and structure of the nucleus. A confirmation of these theories lies in the ability to measure experimentally the forces existing within the field regions of the nucleus of the atom. One of the properties of the nucleus that contributes to this experimental information is the nuclear magnetic moment. In 1946 two independent research groups, one at Harvard[1] and the other at Stanford University,[2] developed new methods for measuring this nuclear moment. Since then measurements have been made on many elements of high natural abundance and these results are in the scientific literature.[3] The data from these various laboratories have not always been in agreement, and several scientists[4,5] have shown that the measured value for the nuclear magnetic moment depends upon the chemical compound and state of the sample.

It is the intent of this research to make precise measurements on several of the nuclides and to present the design data on the equipment used in making these measurements. The system to be described was constructed with this purpose in mind.

Since the construction of this equipment several instruments capable of precision measurements have been built at other laboratories. Three of the major laboratories use the system of nuclear absorption[6] and three others the system of nuclear induction.[7] Most of the investigations at the other laboratories have been directed towards the study of chemical and nuclear shielding effects and not primarily the measure-

2

ment of nuclear moments. Sufficient results are now available to determine that both systems have the same ultimate precision.

An electrically charged particle undergoing a rotation will possess an angular momentum and a magnetic moment. In atomic physics the unit of the magnetic moment is $(e\hbar/2mc)$ and is called the Bohr magneton. The unit for the magnetic moment in nuclear physics is $(e\hbar/2M_pc)$ and is called the nuclear magneton and is designated by the symbol μ. In general all nuclear moments are most easily referred to that of the simplest nuclide of hydrogen which has only one proton because the proton magnetic moment has been measured very precisely by several methods. The methods of nuclear magnetic resonance do not measure the nuclear magnetic dipole moment directly, but instead determine a value for the ratio of the nuclear magnetic moment to the spin angular momentum; hence, to determine the magnetic moment of a nuclide the spin (angular momentum) must be known. This ratio is commonly called the gyro-magnetic ratio although more properly should be called the magneto-gyric ratio. Most spin values have been determined by other methods, although it is possible to determine the spin by means of intensity measurement of the nuclear magnetic resonance.[8,9] Measurement of moments is limited to elements exhibiting an angular momentum. All nuclei thus far studied having an even number of protons and of neutrons possess zero spin in the ground state since there is a pairing of oppositely directed spins for the respective nucleons; odd-odd nuclei necessarily have integral values of spin, while for even-odd and odd-even species the resultant spin is half-integral. Since odd-odd nuclei are rare, this then with but

few exceptions limits the measurement of the nuclear magnetic moment to nuclides having odd mass numbers.

The results of the measurement of nuclear moments are useful in developing and verifying the theories of nuclear structure. If certain models are chosen for the nuclear configurations it is possible by means of quantum theory to estimate the value for the nuclear magnetic moment. Measured values for the magnetic moment of several nuclides have fallen within the limits of the predicted value as calculated from certain of these nuclear shell models; however, many discrepancies still remain.

NOMENCLATURE

e = charge on the proton

$\hbar$ = $(2\pi)^{-1}$ times the Planck constant

m = mass of the electron; magnetic quantum number

c = velocity of light in vacuum

M_p = mass of the proton

$\bar{a}$ = angular momentum vector

g = nuclear g-factor

μ_o = $(e\hbar)/(2M_pc)$ = nuclear magneton

μ = gI = nuclear magnetic moment, the number of nuclear magnetons

γ = $g\mu_o/\hbar$ = ratio of angular Larmor frequency to magnetic field; $\mu/I\hbar$

I = spin quantum number in units of $h/2\pi$

μ_n = magnetic polarization vector

ω_o = angular frequency of Larmor precession, $2\pi\nu_o$

H = magnetic field

L = torque vector

H_o = constant magnetic field vector

$\overline{M}$ = nuclear magnetization vector density

χ = paramagnetic susceptibility

χ_o = constant field value of χ, see Equation 10

N = number of nuclear magnetic moments per unit volume

k = Boltzmann constant

T = absolute temperature, degrees Kelvin

H_o^* = the value of the applied field at resonance

H_1 = a rotating magnetic field, half amplitude of the oscillating field

θ = angle formed between $\overline{M}$ and the steady field direction

T_1 = spin-lattice (thermal or longitudinal) relaxation time

T_2 = spin-spin (transverse) relaxation time, inverse line width

M_o = equilibrium value of z component of nuclear magnetization

ψ = conversion constant for ν in cps, H in gauss, μ in nuclear magnetons

WWV = National Bureau of Standards standard frequency ratio transmissions

Q = figure of merit for a coil; $\omega L/R$

n = volume density of nuclei

δ = deviation of H_o (or ω) from the resonance in units of H_1

B = magnetic induction vector

F = flux linkage due to magnetization density

H_m = magnetic modulating field

ν = frequency of radiation, $\omega/2\pi$

H_{loc} = magnetic field produced at lattice by neighboring nuclear moments

χ', χ'' = real and imaginary parts of $\chi = \chi' - i\chi''$

$\Delta\omega$ = $(\omega - \omega_0)$, deviation in ω from resonance

A = power absorbed per unit volume

λ = sample volume

NUCLEAR RESONANCE THEORY

If a nucleus in its ground state has an angular momentum $\bar{a}$, we can describe the resulting nuclear magnetic dipole moment vector as

$$\bar{\mu} = g(e/2M_p c)\,\bar{a} = g\mu_0\,\bar{a} = \gamma\bar{a} \tag{1}$$

where g is the dimensionless gyromagnetic ratio, and γ is the ratio of the nuclear magnetic moment to spin angular momentum. The spin quantum number I of the nucleus is equal to $1/\hbar$ times a_h, the largest component of $\bar{a}$ in a specified direction, in our case in the direction of the applied static magnetic field H, for which $\bar{a}$ can take on discrete values

$$a_h = m\hbar, \text{ where } m = I, I-1, \ldots\ldots -I+1, -I. \tag{2}$$

If the nucleus having a magnetic dipole moment $\bar{\mu}_n$ is placed in the magnetic field, a torque $(\bar{\mu}_n \times \bar{H})$ is exerted upon the dipole and the time rate of change will be

$$d\bar{a}/dt = \bar{\mu} \times \bar{H} \tag{3}$$

and upon substituting for $\bar{\mu}$ we find

$$d\bar{a}/dt = \gamma\bar{a} \times \bar{H} = -\gamma\bar{H} \times \bar{a} \tag{4}$$

It is easily seen that this is the equation of motion for a vector $\bar{a}$ precessing with angular velocity $\omega_0 = -\gamma H$ if one considers the relationships shown in Figure 1 where a vector $\bar{a}$ is rotating about an axis with angular velocity ω_0. One sees that $d\bar{a}$ is equal to $\omega_0 \times \bar{a}\,dt$,

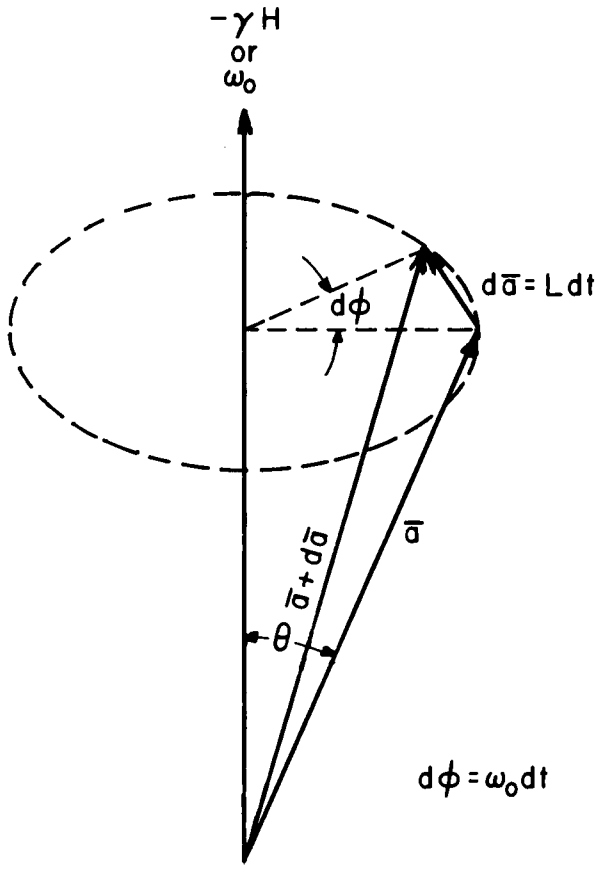

$$d|a| = |a| \sin\theta \, d\phi = |a| \sin\theta \, (\omega_o dt) = \omega_o \times |a| dt$$

Figure 1. The relationship between classical mechanics and the nuclear magnetic moment and spin interactions

but if $\bar{a}$ is the angular momentum vector for a particle, then $\frac{d\bar{a}}{dt}$ is the torque, L, which for the nuclear particle is $-\gamma H \times \bar{a}$. Therefore

$d\bar{a}/dt = -\gamma\bar{H} \times \bar{a} = \bar{\omega}_o \times \bar{a}$, and

$$\bar{\omega}_o = -\gamma \bar{H} \tag{5}$$

The angular frequency ω_o is called the Larmor precession frequency.

We now define the component of $\bar{\mu}_n$ in the direction of the applied field as the magnetic moment μ. If nuclei possessing such a moment and a nuclear spin I, are subjected to a steady magnetic field H_o directed along the Z-axis, there will be a coupling of their spin with the magnetic field and a tendency to align themselves in the field with positions corresponding to the quantized 2I + 1 Zeeman energy levels. The energies separating successive levels will be equal except for quadrupole effects,† and the energy difference will be found to be $h\nu = \hbar\gamma H$. This energy difference, upon application of an exciting field, will give rise to an absorption of energy at the angular frequency $\omega = 2\pi\nu$, which for values of magnetic field ($\sim 10^4$ gauss) falls in the megacycle radio-frequency region. The nuclear moment vector will precess around H_o with the Larmor angular frequency ω_o. If there is then supplied perpendicular to the steady magnetic field H_o a rotating magnetic field H_1, where $H_x = H_1 \cos \omega t$, $H_y = H_1 \sin \omega t$, $H_z = 0$, a new torque ($\bar{\mu}_n \times H_1$) will be exerted upon $\bar{\mu}_n$. If the rotating frequency ω is the same as the Larmor precession frequency ω_o, the angle between H_o and $\bar{\mu}_n$ will change because of

---

† If a nucleus has a non-zero electric quadrupole moment ($I > \frac{1}{2}$) and is situated in an electric field with a non-vanishing gradient ∇E, each of the Zeeman levels will be perturbed and the single absorption line of frequency ω will be split into 2I components. Volkoff, A. B., Canadian Journal of Physics, volume 30, May 1, 1952, page 270.

the in-phase character of the torque, and $\bar{\mu}_n$ will tend to tip towards a new energy state. If $\omega \neq \omega_o$ the average effect will be zero and no tipping tendency will occur. The rotating field H_1 can be easily established by using an oscillatory field $H_x = 2H_1 \cos \omega t$, $H_y = 0$, $H_z = 0$ which can be considered to be the sum of two fields rotating about the Z-axis in opposite directions:

$$\overset{\curvearrowright}{H_x} = H_1 \cos \omega t \qquad \overset{\curvearrowleft}{H_x} = H_1 \cos \omega t \tag{6}$$

$$\overset{\curvearrowright}{H_y} = H_1 \sin \omega t \qquad \overset{\curvearrowleft}{H_y} = -H_1 \sin \omega t \tag{7}$$

$$\overset{\curvearrowright}{H_z} = 0 \qquad \overset{\curvearrowleft}{H_z} = 0 \tag{8}$$

If the frequency of oscillation of the applied field is $\omega = \omega_o$, then one of the components will follow the precessing vector $\bar{\mu}_n$ and produce energy transitions; the other component will be far off resonance and can be neglected. This theory as now applied to the nuclear induction method is an extension of the original work of Rabi[10] and his co-workers in the measurement of nuclear moments by the molecular beam resonance method.

Let us consider the magnetization effects in a macroscopic sample. In the presence of a steady magnetic field we will find that the orientation of the individual nuclei due to their various energy levels produces a resultant vectorial magnetic polarization $\bar{M}$. The magnetization in the direction of the field can be expressed by

$$\bar{M} = \chi \bar{H}, \tag{9}$$

where χ is the nuclear paramagnetic susceptibility given by the relation

$$\chi_o = \frac{I+1}{3I} \quad \frac{N\mu^2}{kT} \tag{10}$$

The magnetization then becomes

$$\bar{M} = \frac{NI(I+1)\gamma^2\hbar^2\bar{H}}{3kT}, \quad H\mu \ll kT \tag{11}$$

We are interested in the various components of $\bar{M}$, in particular M_z, the component along the field direction, and M_y, the component we shall detect.

From Equations 3, 4, and 5 we can write an expression for the rate of change of the macroscopic polarization vector (the magnetic moment per unit colume) for a sample, such that

$$\frac{d\bar{M}}{dt} = \gamma\left[\bar{M} \times \bar{H}\right] \tag{12}$$

If certain assumptions are now made that the oscillatory field H_1 is much smaller than the steady field H_o ($H_1 \ll H_o$), and that the circular frequency ω of the oscillatory field is in the neighborhood of the resonance frequency ω_o such that $|\omega - \omega_o| \ll \omega_o$, where $\omega_o = \gamma H_o$ it is possible to find a special solution to Equation 12 where $\bar{M}$ will be found to precess around H_o at a steady angle θ with an angular frequency ω.

The three components of $\bar{M}$ can be written as:

$$M_x = |M| \sin\theta \cos\omega t \tag{13}$$

$$M_y = |M| \sin\theta \sin\omega t \tag{14}$$

$$M_z = |M| \cos\theta \tag{15}$$

where $|M|$ is the magnitude of $\bar{M}$. With H_x given by Equation 6, the angle θ is found to be such that

$$\tan\theta = \frac{\gamma H_1}{\gamma H_o - \omega} = \frac{H_1}{H_o - H_o^*} = \frac{\gamma H_1}{\omega_o - \omega} \tag{16}$$

where $H_o^* = \omega/\gamma$ is the field whose Larmor frequency is ω. Equation 16 shows that if H_o is greatly different from H_o^*, the angle θ will be small because H_1 is small.

Resonance conditions can be achieved by varying either ω or H_o and at resonance $H_o = H_o^*$ (or $\omega = \omega_o$) the angle θ will be found to be 90

degrees. This means that

$$M_x = |M| \cos \omega_o t \tag{17}$$

$$M_y = |M| \sin \omega_o t \tag{18}$$

$$M_z = 0 \tag{19}$$

and that $\overline{M}$ is perpendicular to the steady field H_o and rotates about it at the Larmor frequency ω_o.

For $\omega \neq \omega_o$ but where ω is in the neighborhood of ω_o the components of $\overline{M}$ are found by substituting Equation 16 in the equations for the components Equations 13, 14, and 15. If we permit $\cos \theta = \delta = (H_o - H_o^*)/H_1$ to be the deviation of H_o from its resonance value H_o^* in units of $|H_1|$, we can rewrite Equations 17, 18, and 19 to be

$$M_x = M \frac{\cos \omega t}{(1 + \delta^2)^{\frac{1}{2}}} \tag{20}$$

$$M_y = M \frac{\sin \omega t}{(1 + \delta^2)^{\frac{1}{2}}} \tag{21}$$

$$M_z = M \frac{\delta}{(1 + \delta^2)^{\frac{1}{2}}} \tag{22}$$

This rotating magnetic field is used to induce a voltage in a coil having its turns in the X-Z plane, and the method is therefore termed "nuclear induction."

The simple solution to Equation 12 as given is not that of a practical nuclear case but is that for a system of free nuclear spins. To consider the conditions of a practical situation cognizance must be taken of the interactions occurring between the nucleus and the lattice, and between adjacent spins. In the simplified case considered, M_z was found to be zero at resonance. In the case where other interactions are also considered this is not true in general. The effects of these in-

teractions influence the equations of motion of $\overline{M}$ by introducing extra terms that contain the so-called relaxation times. For a further discussion of the origin and effects of these terms reference is made to the article of Pake.[11] The spin-lattice relaxation time T_1 is related to the period required for a nuclear thermal equilibrium to be achieved and is a measure of the time required for the z component of $\overline{M}$ to attain realignment in the steady field. In addition to the applied fields, there are local fields due to neighboring nuclei. Interactions with these local fields tend to induce additional energy changes. These interactions are called spin-spin collisions and cause a destruction of the phase relationship between the nuclear moment components and are associated with a relaxation time T_2 which is determined by the spread in local magnetic field values at the nucleus. Usually one can assume T_2 to be less than T_1. Additional comments on relaxation times will be found in Appendix I and in reference 6.

Bloch[7] has further solved a set of classical equations of motion for the components of $\overline{M}$ obtained by modifying Equation 12 for the spin-spin and spin-lattice coupling. The expression for the components of $\overline{M}$ including these modifications becomes

$$\frac{dM_x}{dt} = \gamma\left[M_yH_o + M_zH_1 \sin\omega t\right] - M_x/T_2 \tag{23}$$

$$\frac{dM_y}{dt} = \gamma\left[M_zH_1 \cos\omega t - M_xH_o\right] - M_y/T_2 \tag{24}$$

$$\frac{dM_z}{dt} = \gamma\left[-M_xH_1 \sin\omega t - M_yH_1 \cos\omega t\right] + (M_o - M_z)/T_1 \tag{25}$$

It is convenient to introduce two new variables u and v through the relationship

$$M_x = u \cos \omega t - v \sin \omega t \tag{26}$$

$$M_y = \mp(u \sin \omega t - v \cos \omega t), \text{ sign dependent upon sign of } \gamma \tag{27}$$

A complete solution of these equations is given by Bloch[7] and details may be found in Pake.[11] The resultant nuclear moment $\bar{M}$ is resolved into three components

$$M_z = \frac{1 + T_2\Delta\omega)^2}{1 + (T_2\Delta\omega)^2 + (\gamma H_1)^2 T_1 T_2} \cdot M_o \tag{28}$$

in the Z direction,

$$u = \frac{\gamma H_1 T_2 \ (T_2\Delta\omega)}{1 + (T_2\Delta\omega)^2 + (\gamma H_1)^2 T_1 T_2} \cdot M_o \tag{29}$$

parallel to the effective component of H_1, and

$$v = \frac{-\gamma H_1 T_2}{1 + (T_2\Delta\omega)^2 + (\gamma H_1)^2 T_1 T_2} \cdot M_o \tag{30}$$

orthogonal to M_z and leading H_1 by 90 degrees, where $\Delta\omega = \gamma H_o - \omega = \omega_o - \omega$ and H_1 is half amplitude of the oscillatory field. It is assumed that $M_o = M_z$ for this particular solution. Then M_y can be written upon substitution of Equation 29 and 30 into Equation 27 as

$$M_y = \tfrac{1}{2}\omega_o \chi_o T_2 \left[\frac{2H_1 \cos \omega t - 2T_2\Delta\omega H_1 \sin \omega t}{1 + (T_2\Delta\omega)^2 + (\gamma H_1)^2 T_1 T_2} \right] \tag{31}$$

where χ_o is given by Equation 10.

Since our detector coil is oriented along the Y axis, M_y is the physically observable quantity of interest. It can be seen from Equation 31 that M_y has components both in-phase and out-of-phase with the driving field H_1. The component that one observes experimentally depends upon whether the phase of the leakage voltage signal (used for homodyning and detection as later explained) is in-phase, at 90 degrees,

or at some other phase angle with respect to the oscillatory field H_1. Under conditions where the resonance is approached by a slow variation of H_o or ω the v component corresponds to an absorption and gives a symmetrical curve and the u component corresponds to a dispersion and gives an anti-symmetrical curve. A further discussion of these phase relationships and the complex susceptibility is included in Appendix II.

For the nuclear induction system which utilizes the voltage induced by this resonating magnetic field, it is desirable to have u as large as possible, since it is this component of M_y that contributes to the dispersion and the induction signal. Its largest value occurs for

$$\Delta\omega = \frac{\left[1 + (\gamma H_1)^2 T_1 T_2\right]^{\frac{1}{2}}}{T_2} \tag{32}$$

when it has the maximum value

$$u_{max} = \frac{\gamma T_2 H_1}{\left[1 + (\gamma H_1)^2 T_1 T_2\right]^{\frac{1}{2}}} \cdot M_o \tag{33}$$

This maximum increases monotonically with H_1, and for $(\gamma H_1)^2 T_1 T_2 \gg 1$ becomes

$$u_{max_{max}} = \frac{1}{2}\left[\frac{T_2}{T_1}\right]^{\frac{1}{2}} \cdot M_o \tag{34}$$

These solutions indicate that for the nulcear induction signal to be as large as possible H_1 should also be as large as possible. However excessively large fields for H_1 introduce practical problems in the construction of suitable driving and detecting coils and H_1 is usually limited to a relatively small value compared with the steady magnetic field H_o. One can also consider the v term in Equation 26, since it is this

quantity that determines the out-of-phase portion of M_x and the in-phase portion of M_y. It is the v term that is a measure of the absorption component of the signal. From Equation 31 we find that for resonance conditions, $\Delta\omega = 0$, it has a maximum

$$v_{max} = \frac{\gamma H_1 T_2}{\left[1 + (\gamma H_1)^2 T_1 T_2\right]} \cdot M_o \tag{35}$$

and does not increase monotonically with H_1 as does u_{max} but decreases for extremely large values of H_1. The best choice to limit saturation is

$$(\gamma H_1)^2 T_1 T_2 = 1 \tag{36}$$

and then it also gives for a maximum

$$v_{max_{max}} = \frac{1}{2}\left[\frac{T_2}{T_1}\right]^{\frac{1}{2}} \cdot M_o \tag{37}$$

In the practical case it is possible to have both the u and v "modes" affect the detected signal, since a slight disparity in the phase of the leakage or driving field H_1 will alter the effect of the induced signal as will be later discussed.

THE NUCLEAR INDUCTION METHOD

The preceding section pointed out that nuclei subjected to a steady magnetic field and a high frequency alternating field are forced into energy transitions which give rise to a radiation of energy in the form of a magnetic induction field in the radio-frequency spectrum. A method is described whereby these radiations can be detected and measured. Bloch, Hansen, and Packard[12] have described a system which they have called "nuclear induction." This system utilizes a pair of crossed or-

thogonal coils for exciting the nuclei and detecting the induced emf. The sample is surrounded by one coil which has its terminals connected to a sensitive detecting system. A second coil adjusted for minimum coupling with the detector coil impresses a high frequency alternating magnetic field upon the sample. Both coils and the sample are surrounded by a steady magnetic field oriented perpendicular to the plane of the two coils. Radio-frequency energy of the proper frequency causes the nuclear polarization to be altered from its equilibrium position and to rotate in step with the driving field and induce an emf in the detecting coil.

Before considering the design of an apparatus suitable for detecting this induction it is desirable to know something about the required magnetic field values, the frequency range over which the equipment must operate, the magnitude of the impressed field H_1, the characteristics of the amplifiers and recording system, and the amplitude of signal that one might expect from the nuclear sample.

First, the character of the signal expected should be considered since this will determine the feasibility for the design of the system and will lead to values for the necessary parameters. As an example, reference is made to the most ideal nuclide, the proton, whose magnetic moment is 2.7926 nuclear magnetons, and whose spin is $\frac{1}{2}$. Thus the gyromagnetic factor is 5.5852; it is the largest γ factor known. Since the spin is $\frac{1}{2}$ only $2I + 1 = 2$ orientations are permitted for the nuclear polarization in a magnetic field, parallel and anti-parallel. For a sample containing one cm^3 of water at room temperature ($T = 291^\circ$ K.) and having $n = 6.9 \times 10^{22}$ nuclei per cm^3, the susceptibility is calcu-

lated from Equation 10 to be $\chi = 3.4 \times 10^{-10}$. For a magnetic field of 5000 gauss the magnetic moment density $\overline{M} = \chi \overline{H}$ is found to be 1.7×10^{-6} gauss. The apparatus does not observe $\overline{M}$ itself, but detects the rate of change of the induction $B_y = 4\pi M_y$. The frequency at which the apparatus must operate can be determined from the original expression for $h\nu$. This can be rewritten in a different form where a constant ψ has been added to convert to the most commonly used units of cycles per second, gauss, and nuclear magnetons. The frequency is found to be

$$\nu = \gamma H \psi \tag{38}$$

where $\psi = 0.76229 \times 10^3$. For a field of 5000 gauss, ν then must be 21.3×10^6 cps. This frequency is a linear function of magnetic field strength unless perturbed by electric quadrupole effects and doubling or halving the magnetic field will still permit the radiations to lie in a practical radio-frequency range for a crossed coil system. Certain advantages are obtained from using the highest magnetic field possible and these will appear later in a discussion of the voltage available from the nuclear magnetization. If the sample takes the form of a sphere, the flux linkage through a turn about the equatorial circle is equal to that caused by a magnetic field of magnitude $8\pi/3$ times the moment density.[13] For this case the linkage through such a single turn will be the same as if a uniform field of 1.43×10^{-6} gauss were linking the turn. Suppose the spherical sample is placed in a coil oriented along the Y axis and in a steady magnetic field of 5000 gauss in the Z direction, then by means of a split coil, orthogonal to these two axes, an alternating field $H_x = 2H_1 \cos \omega t$ is applied. The signal from the nuclear polarization will be present in the detector coil only near a resonance. The

amplitude for the components of this polarization $\overline{M}$ as previously shown will be

$$M_x = \frac{M}{(1+\delta^2)^{\frac{1}{2}}} \cos \omega t \tag{20}$$

$$M_y = \frac{M}{(1+\delta^2)^{\frac{1}{2}}} \sin \omega t \tag{21}$$

$$M_z = \frac{M}{(1+\delta^2)^{\frac{1}{2}}} \tag{22}$$

where

$$\delta = \frac{H_o - H_o^*}{H_1} \tag{39}$$

is the deviation of H from its critical value, H_o^* in units of the half amplitude of H_1. A curve of the function $1/(1+\delta^2)^{\frac{1}{2}}$ is given as Figure 2. The ordinate is proportional to M_y, the component of $\overline{M}$ in the direction of the detector coil and thus to the amplitude of the induced voltage. To induce transitions successfully the driving field H_1 should be larger than the internuclear fields. If 1 gauss is chosen as an acceptable value for H_1, the field H_x will be 2 gauss and the problem becomes one of detecting a field of about 1.5×10^{-6} gauss in a field of the same frequency but of a magnitude 1.33×10^6 times larger. Upon comparing the field component M_y with the driving field H_x it is found that a time quadrature relationship exists.

Consider now methods whereby the voltage appearing at the terminals of our detector coil can be increased. The largest sample volume capable of being enclosed by the coil will provide the greatest quantity of nuclei and hence the largest moment density $\overline{M}$. Since the voltage at the coil terminals is proportional to the total flux-linkage turns, the

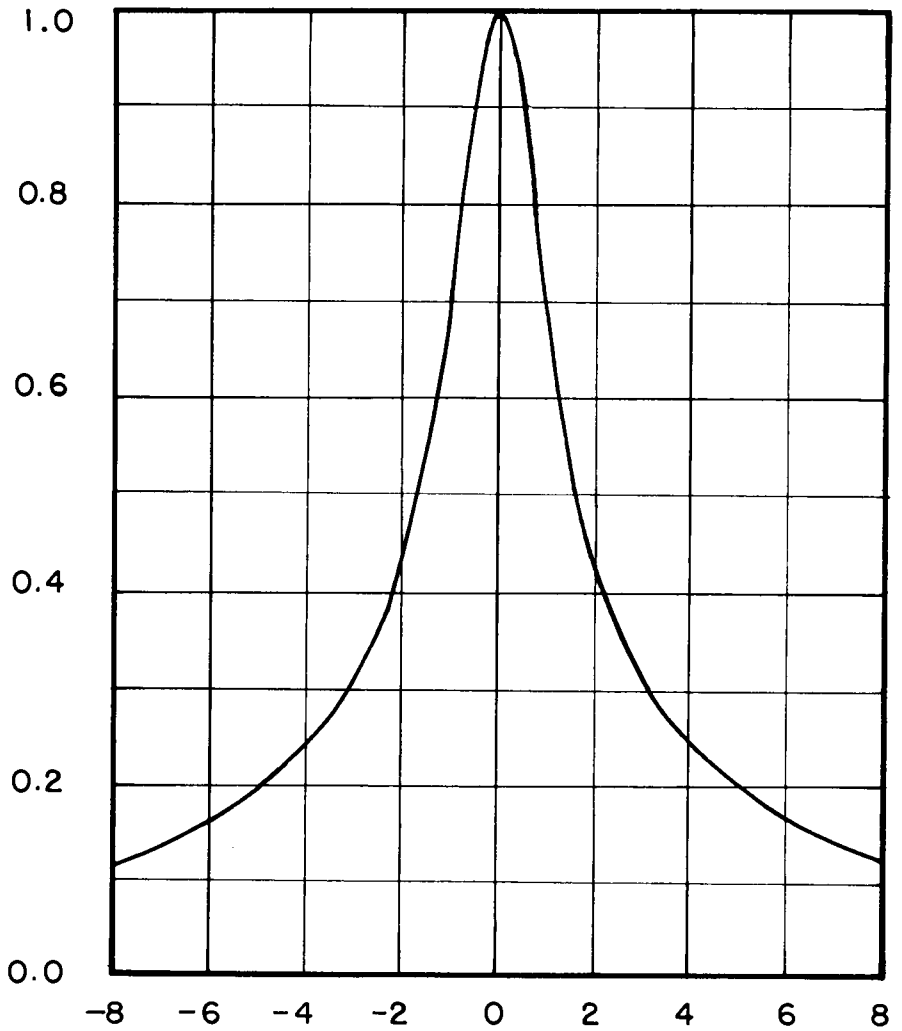

Figure 2. The amplitude of generated voltage for rapid passage when using a sweeping field $H_m \cos \omega_m t$. The ordinate is proportional to the amplitude of M_y. The abscissa is the variation in H_0 from the resonant value H_0^* in units of the half amplitude of H_1

coil can be a multiplicity of turns, and in addition can be tuned to resonate at the emission frequency 21.3 mc by an external capacitor. The detector coil gain is increased by the Q of the resonated LC network. Distributed capacity will limit the amount of inductance that can be used and still maintain resonant conditions. A judicious choice must be made between the interlinking factors of coil diameter, length, and turns, since they affect the Q and the sample size directly. Resonating the detector coil will not improve the inherent signal-to-noise ratio, but will increase the observed signal-to-noise ratio by the increased signal-to-tube noise at the input stage. A coil suitable for holding a sample of a few cubic centimeters volume can be constructed with a Q between 75 and 150. The thermal (Brownian) noise from such a coil should be less than 1 microvolt in a 5 kc band range and could be further decreased by limiting the band-width or increasing the Q.

The magnitude of the voltage present at the detector network terminals can now be calculated. The induction will be

$$B_y = 4\pi M_y \tag{40}$$

and the flux linkage will be

$$F = 4\pi NAM_y \tag{41}$$

The voltage generated is the rate of change of this flux linkage and will be

$$V = \frac{1}{c}\frac{dF}{dt} \quad \frac{1(I)(I+1)\hbar^2\gamma\omega^2\cos\omega t}{\pi c(3kT)(1+\delta^2)^{\frac{1}{2}}} \lambda Q\, 10^{-8} \tag{42}$$

and the root-mean-square voltage is

$$V_{rms} = \frac{1}{\sqrt{2}} \quad \frac{4\pi M}{(d^2+h^2)^{\frac{1}{2}}} \quad NQ\omega\lambda 10^{-8} \tag{43}$$

where d is the coil diameter, h the coil length (both in cm), and λ the sample volume. A coil having 22 turns of #20 enameled wire with a diameter of 1.9 cm and a length of 1.27 cm will have a calculated free air Q of 380.[‡] Because of necessary shielding this will drop to a value near 200. If a sample volume of 3 cm^3 is assumed, the voltage expected at the coil terminals will be 0.12 volt, a very sizeable signal that can be detected without further radio-frequency amplification. Unfortunately not all nuclei provide such a large signal. For example, if the voltage is calculated for the deuterium resonance occurring in a similar sized sample of normal tap water (0.0156 percent D_2O) at the same magnetic field one finds only 1.8 microvolts available. This is nearing the limits of practical circuit noise and is a measure of the sensitivity in the best equipment. This voltage could be increased by a factor of three of four by using a larger number of turns on the detector coil providing the Q was not decreased. Doubling the magnetic field will increase the signal another fourfold and one can then expect the signal to be about 2.9 microvolts which should exceed the thermal noise of the coil. Since both $\bar{M}$ and ω vary directly with the magnetic field H the detector coil voltage varies as the square of the magnetic field for a given nuclide.

Consider now the effects of the strong field $H_x = 2H_1 \cos \omega t$. This is somewhat more than 10^6 times larger than the nuclear induction field and it is necessary to reduce the coupling of this field with the detector coil by a large factor to prevent saturation of the early am-

---

[‡]A complete discussion of coil design for optimum Q and form size can be found in reference 14, pp. 463,475.

plifier stages. Under ideal conditions a reduction of 10^4 requiring an angular orientation of the orthogonal coils to 20 seconds could be achieved, but a reduction of 10^6 would require an angular adjustment to 10^{-6} radian or 0.2 second. Even were such an adjustment possible, couplings through distributed capacity, coil non-uniformity, etc. would prevent this much decoupling. Fortunately a method is available whereby this coupled leakage flux can be utilized.

A common method for increasing the selectivity of a system and at the same time reducing the band-width and thereby decreasing noise is the use of the superheterodyne principle, where some lower intermediate frequency is chosen for further amplification and detection. In this apparatus this intermediate frequency is chosen to be zero and the leakage signal, with modification becomes the local oscillator voltage source. In order to make use of the superheterodyne principle it is desirable to have the input signal modulated. This is done by adding to the steady magnetic field a considerably weaker oscillating field $H_z = H_m \cos \omega_m t$. This weaker field causes the steady field to be swept back and forth across the resonance value H_o^* at a constant repetition rate and the resulting induction from M_y is turned on and off periodically.

As has been pointed out, the leakage signal from H_1 and the signal generated by M_y are 90 degrees out of time phase so that if the leakage voltage and the modulated signal are added a resulting phase modulation will be observable but the magnitude change will be small. In order to pass this through an ordinary diode detector the leakage must be shifted in phase by $\pi/2$, and the resulting amplitude changes can then be readily detected.

Four methods are used for adjusting the amplitude and phase of the leakage voltage. The coils are first oriented nearly perpendicular by careful machining of the forms and supports. The fields are then further adjusted for a minimum coupling through tilting the r-f field by moving one section of the H_1 field coil parallel to the Y-axis. This reduces the out-of-phase component of the leakage induced in the detector coil to nearly zero. This component is the one associated with the absorption or the "v mode." Electrostatic coupling between the coils is minimized by the use of a grounded Faraday shield. There yet remains the problem of reducing and adjusting the in-phase component of leakage which continues to couple with the detector coil. This component corresponds to the "u mode" or dispersion of the nuclear induction signals and is the leakage that we use as a local oscillator voltage. This u mode leakage is adjusted through the use of two flux diverting devices, one called a loop# and the other a paddle.$ A schematic of the loop is shown in Figure 3. The turn of the loop which lies in the Y-Z plane is coupled uniformly with the coils producing H_1 regardless of angular position about the X axis; however, the turn perpendicular to this plane changes its degree of coupling with the detector coil in the X-Y plane upon rotation about the X-axis. Balance can therefore be achieved by a continuous rotation of the loop until a minimum of coupling exists between the H_1 transmitter and the detector coils. The loop is

---

#This method was suggested, in correspondence, by Dr. H. E. Weaver, Jr., presently at University of Zurich, who credits F. Western of Varian Associates, San Carlos, California.

$A complete discussion of the action of the paddle is given in reference 12, pp. 477-478.

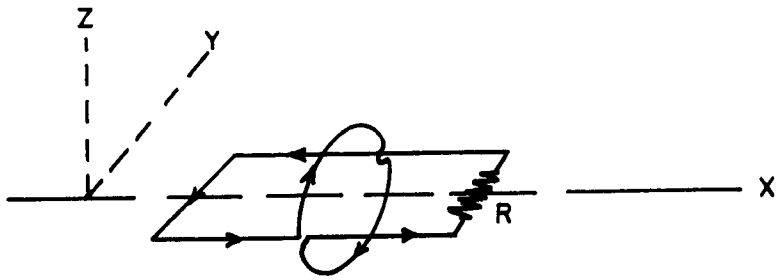

Figure 3. A schematic of the "loop" control. Circulating currents are limited by the resistor R to make the loop impedance predominately resistive

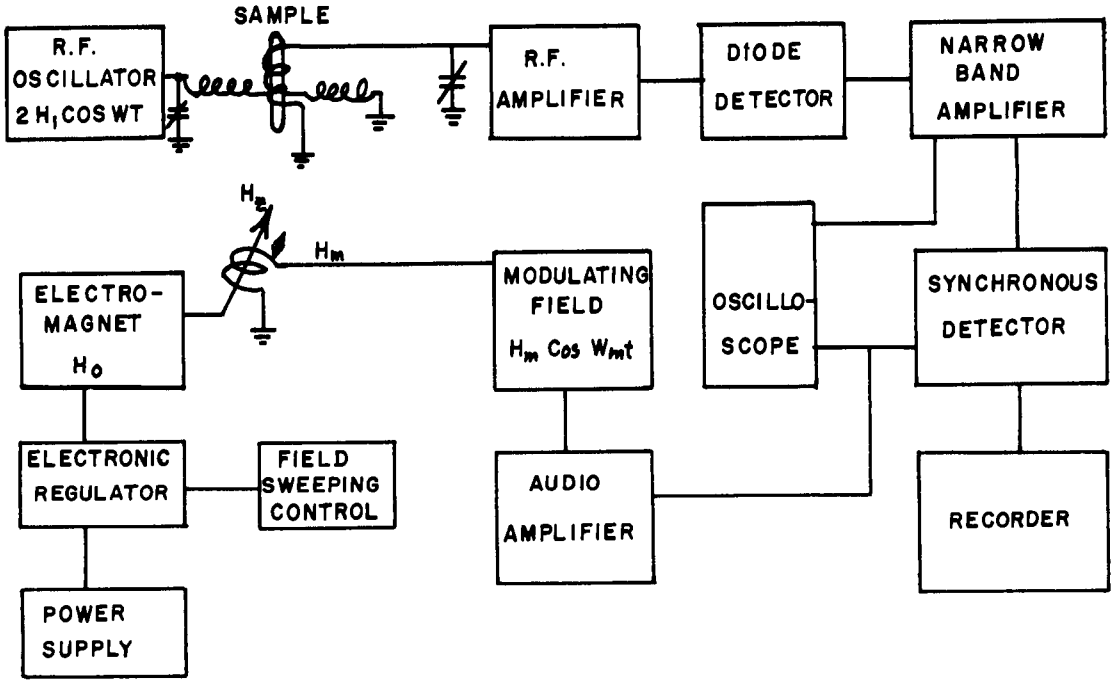

Figure 4. A single line diagram showing the interconnection of the equipment used in performing the nuclear induction experiment

kept predominately resistive through use of a current limiting resistor of about 10 ohms. A vernier adjustment on this minimized coupling is then further made through use of a paddle consisting of a small semi-circular disc of thin copper foil located above the center-line of the H_1 coils. Since radio-frequency flux lines are not permitted to pass through the copper sheet, they are diverted along the y axis and thereby induce in the detector coil an in-phase component of H_1 voltage which can be adjusted for a suitable oscillator voltage level. An additional mechanism is provided for small phase adjustments and oscillator level by injecting into the input stage radio-frequency energy directly from the transmitter through a very small capacity and suitable R-C phase shifters. A single line block diagram illustrating the interconnections of the various equipment is given in Figure 4.

Consider now how further improvements in signal-to-noise ratio may be obtained for extremely small nuclear signals. In general one can improve signal-to-noise through a decrease in band-width of the system. If the modulating field H_m is chosen to be in the low audio frequency range, the output of the detector will be essentially this frequency with higher order harmonics and noise. These can be amplified by high gain audio stages to any desired level. If the sweeping frequency is made to be 100 cps, thereby avoiding a multiple of the 60-cycle line frequency, the equipment can be designed to give optimum gain at this frequency. Elimination of the higher harmonics can be attained through use of a twin-T R-C filter network in the audio amplifier which can provide 15-20 db. of attenuation at 120 cps. The 100-cycle noise minimized signal can then be passed into a phase synchronized detector

which receives its phasing voltage from the same source as the coils producing H_m. The output of the phase synchronous or "lock-in" detector is a direct voltage signal whose polarity is a function of the phase of the incoming signal, and the amplitude of which is proportional to the incoming amplitude if the input signal is smaller than the synchronizing signal. For large nuclear signals the narrow band amplifier and lock-in detector can be by-passed and the resonance displayed directly on an oscilloscope which has its horizontal plates connected to the source of the modulating voltage H_m. A resonance obtained in such a manner is shown in Figure 5 for the pure absorption or "v mode" and in Figure 6 for the dispersion or "u mode." For such a display it is necessary that H_m be large compared with the signal line width, since H_o is maintained at a constant value. In the use of a synchronous detector a modification must be made in the system so that the large steady field may be slowly varied across the resonance value H_o^*. It is possible to achieve the same effect by slowly varying the resonant frequency through the resonant value ω_o and this is frequently done, the choice depending upon which is more convenient. In general, searching for unknowns is performed by varying the magnetic field, whereas precise measurements of nuclear moment ratios usually utilize a constant field and varying radio-frequency. The speed of passage must necessarily be less than the time constant of the lock-in recorder system.

An analysis of the most desirable magnitude for the modulating voltage H_m has been made by Weaver[15] who analyzed the effect of the detecting system on the form of the recorded resonance signal at the output of the synchronous detector. The analysis was carried out on both

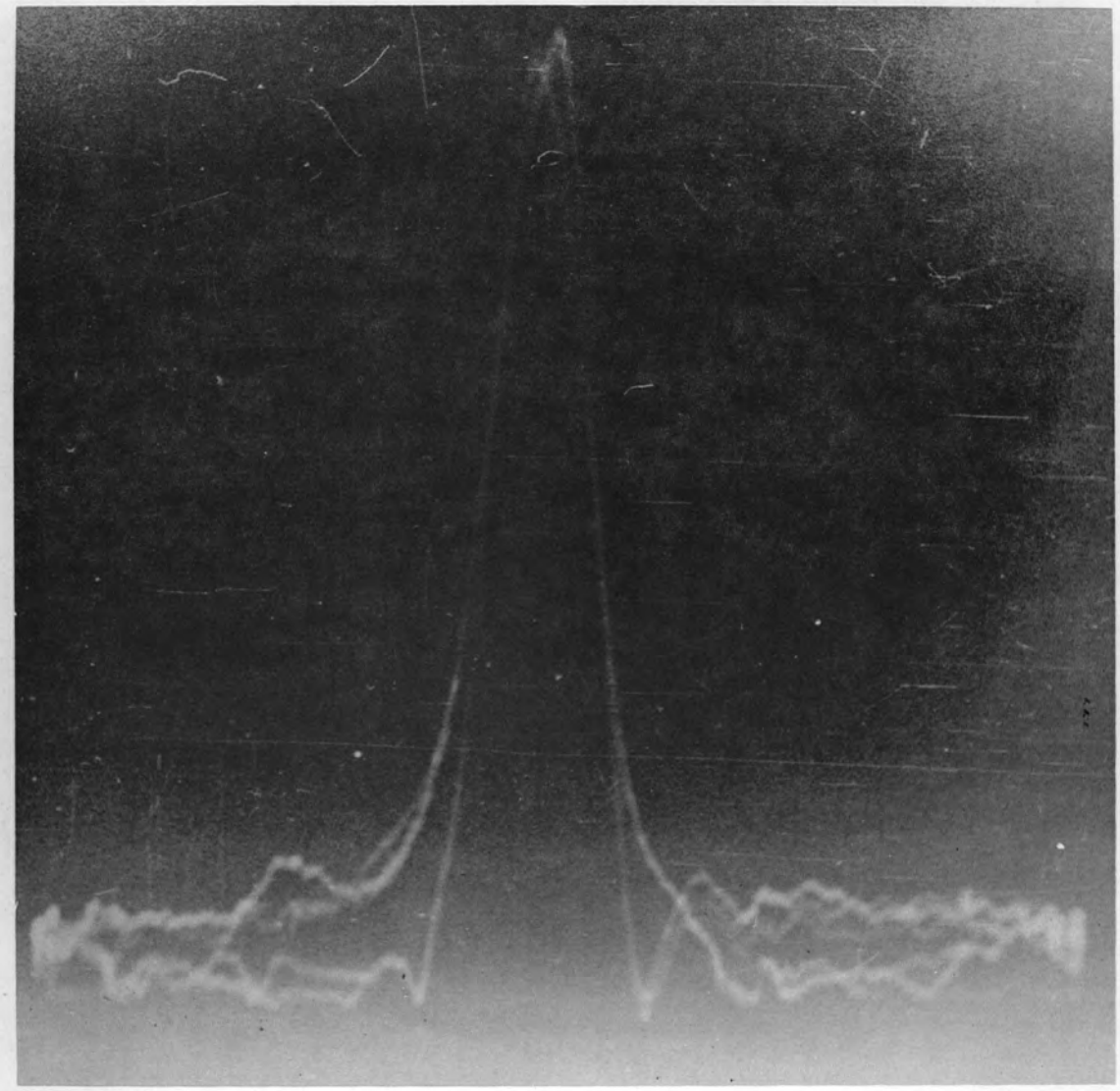

Figure 5. The absorption or "v" mode resonance from protons in a 2ml sample of tap water having 0.1 molar concentration of $MnSO_4$ as magnetic catalyst. The sweeping field H_m is 0.4 gauss

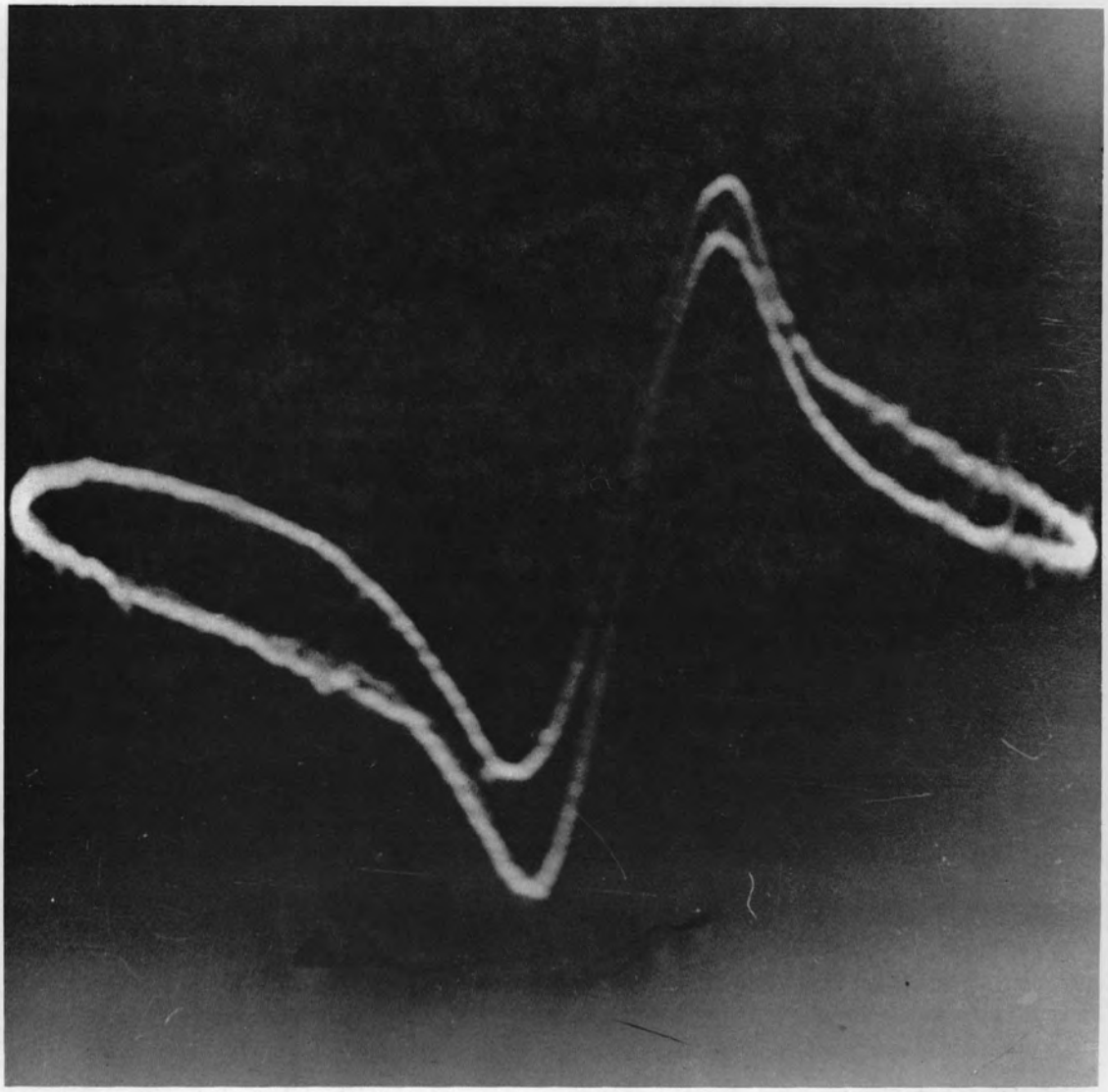

Figure 6. The dispersion of "u" mode signal from protons in 2 ml sample of water containing 0.1 molar $MnSO_4$ as a magnetic catalyst. The sweeping field H_m is approximately 0.25 gauss. The steady field is 2500 gauss

the u and v components and it was found that maximum signals are given for modulating field amplitudes of the order of the natural line width. Thus when searching for unknowns a large modulating amplitude should be used. For conditions of slow passage where a picture of the true line width is desired for determining spin or T_2, the modulating field should be small compared with the natural line width. It is interesting to note that direct oscillographic display gives the absorption and dispersion components directly, whereas the use of a synchronous detector gives the derivative plot of these same functions and the amplitudes are no longer necessarily comparable with the true signal amplitudes.

The frequency of the modulating field should be low enough that the nuclei have time to "relax" before again passing through a resonant condition. This requires that T_1 and T_2 be less than 0.01 second for a typical case. T_1 is difficult to predict and in many cases is of the order of seconds or even minutes. In general T_1 in solids is too long to permit measurement by these techniques and one is restricted with but few exceptions, notably finely powdered metals, to liquid samples. In liquids it is possible to greatly reduce T_1 by the addition of a quantity of paramagnetic ions which act as catalysts due to the action of their relatively large fields. Such catalysts affect the nuclei being measured only minutely because their Larmor resonance frequencies are far removed from that of the nuclei under examination.

In most cases it is more practical to use a cylindrical sample in the form of a test tube than to provide a spherical shape. This increases the number of nuclei that can be contained in a solenoidal coil of given radius over that of a spherical sample and improves the sample-

to-coil coupling. Figure 7 gives a curve showing the effect of sample shape on signal amplitude for a constant volume sample in the form of a thin hollow cylinder. The optimum coupling occurs for the case where the sample fills the coil volume. Extending the length of the sample more than one coil diameter beyond the coil ends produces little additional effect.

Experimental results have shown that the chemical structure of compounds and molecules affect the local fields at the nucleus. Proctor and Yu[16] first observed this compound dependence in nitrogen compounds and shortly thereafter Dickinson[17] reported similar effects in fluorine. A summary of the reported shifts is given in reference 3 including those determined by the author for vanadium[18] and selenium.[19] These shielding effects vary in magnitude from near zero to as high as 0.156 percent in selenium (H_2SeO_3) which is the largest reported to date. Shielding effects in metals are larger due to the local fields generated by the conduction electrons and vary from 0.02 percent for lithium to 1.5 percent for cesium. The shielding effects produce a shift in the observed frequency of resonance from that of a truly unshielded nucleus. Because of these shielding effects it is extremely important that full details of samples and techniques be given in the publication of nuclear moment data. Many other effects such as beats between nuclei in slightly different fields,[20] nutational transients,[21] and lattice orientation effects[22] are not further discussed.

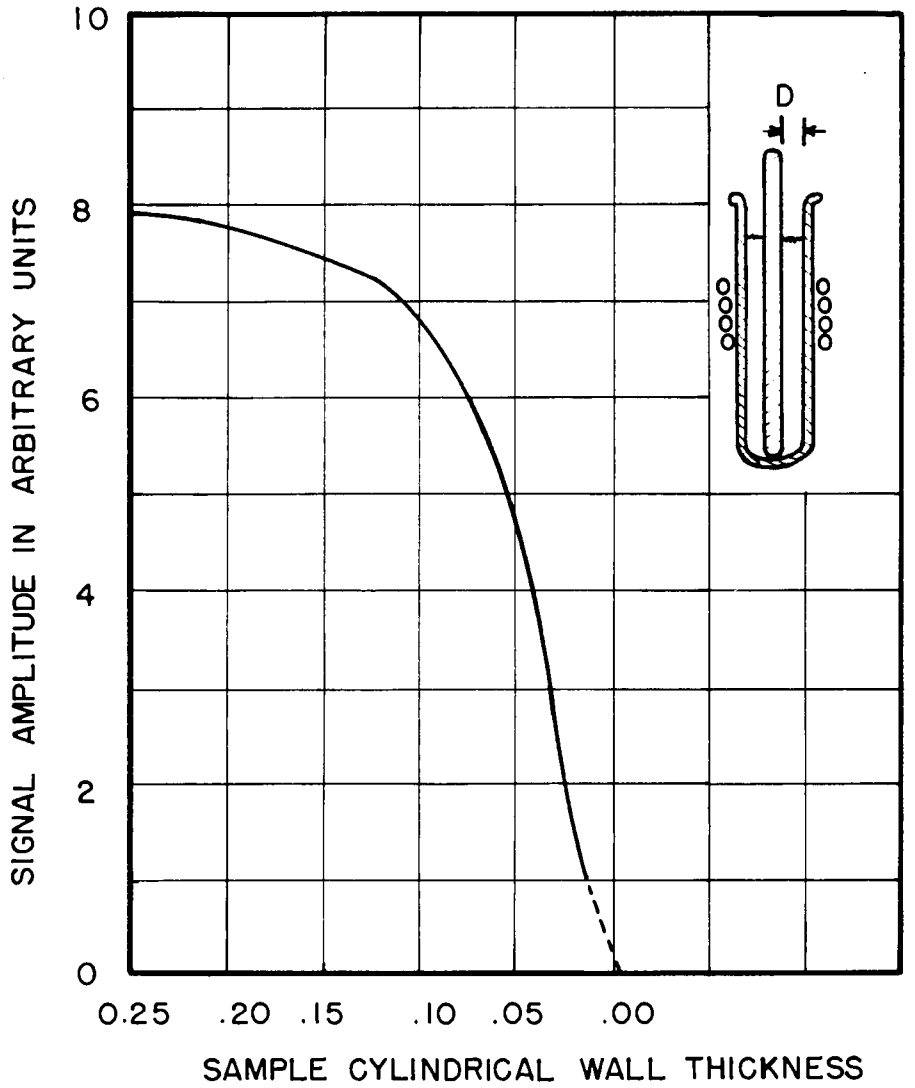

Figure 7. Effect of changing thickness of sample in a holder having the form of a hollow cylinder. This data was taken using the lithium 7 resonance and the sample contained 30 mg of LiCl at a constant volume of 2 cc
D is the cylinder wall thickness

EQUIPMENT DESIGN

High stability of the magnetic field and frequency generating sources is necessary for a precise determination of nuclear magnetic moments. The accurate measurement of magnetic fields in the kilogauss region by direct Amperian means is a difficult task and for convenience one uses an alternate standard for determining the magnetic field. The γ ratio for a nucleus is a constant which permits one to use the magnetic resonance from a measured nuclide as a secondary field strength indicator. When using such a standard the absolute accuracy of all subsequent measurements can be no greater than that of the known standard. Very precise measurement of the γ factor for the proton has been made in calibrated magnetic fields,[23] and in an inverted cyclotron[24] thus providing an excellent nuclear standard. To measure the γ ratios of other nuclides requires a stabilized homogeneous field, a sensitive detector unit, and a means for determining the frequency of resonance, as well as other auxiliary equipment as illustrated in Figure 4. This section deals with the design, operation and characteristics of this apparatus.

THE MAGNETIC SYSTEM

A suitable magnet must not only provide a stable and variable field, but must also provide a high homogeneity throughout the sample volume. To produce such a field an electro-magnet of the double E frame type was constructed having pole pieces with a 12-inch diameter similar to those available from Varian Associates, Palo Alto, California. Pole

caps reduced the diameter to 8 inches at the 1.74-inch gap. The pole caps were hand lapped to within 0.001 inches of parallel and after two years of use no measurable change has occurred.

The cross section of the magnet yoke is 5.25 inches by 12 inches and the magnet is 39 inches high and 33.25 inches wide. It weighs approximately 3500 pounds. The yoke is fabricated from ASTM A107 GR1010-1020 hot rolled steel and the poles and caps from ASTM A107 GR1025 steel. All butt joints are machined surfaces and are held tightly in place by 1.25-7 NC machine stud bolts, the ends of which were milled flat and attached to the poles and yoke by a press fit. Allen head machine screws were used for attaching the pole caps to the pole pieces. These were recessed and covered with plugs of pole cap material. A half-section detail illustrative drawing of the magnet and coil assembly is given in Figure 8, and a photograph of the magnet and its supply in Figure 9.

The coils for the magnet were commercially fabricated and consist of four concentric windings, each having 5000 turns of #17 enameled magnet wire. The resistance of the windings varies in a manner such that the four layer resistances from inside to outside are 94.5, 117.5, 141.5, and 164.5 ohms. A constant turns per winding rather than a constant resistance per winding provides a nearly uniform ratio of heat generation to cooling surface for each winding. In normal use the windings are series connected and present a resistance to the external circuit of 517 ohms at 23° C. The two coils are then series connected. Each coil has approximately 101,000 feet of wire or 640 lbs of copper. Each winding is cooled by a concentric layer of 3/16-inch copper tubing

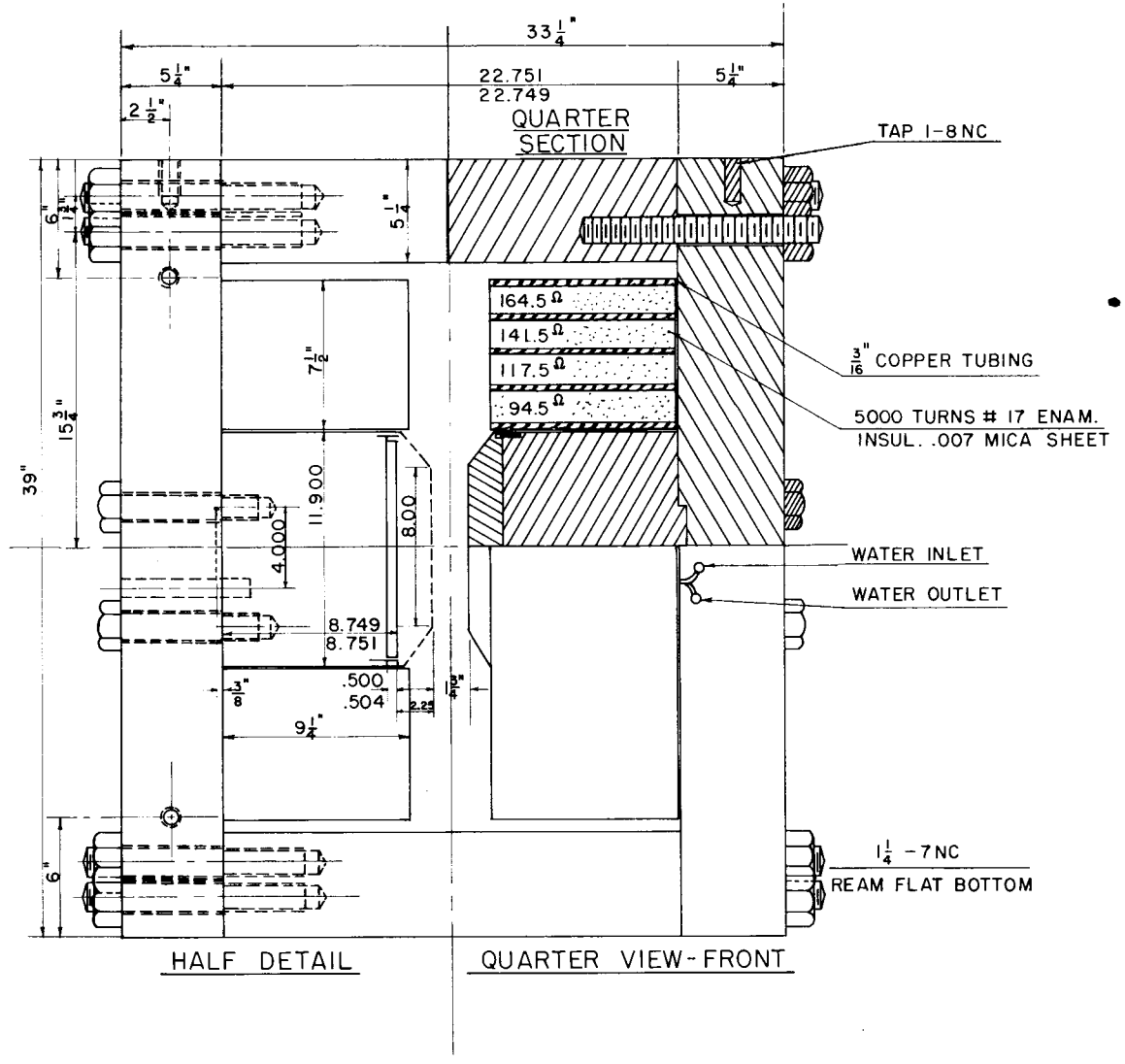

Figure 8. Detail, section, and quarter-view of electromagnet

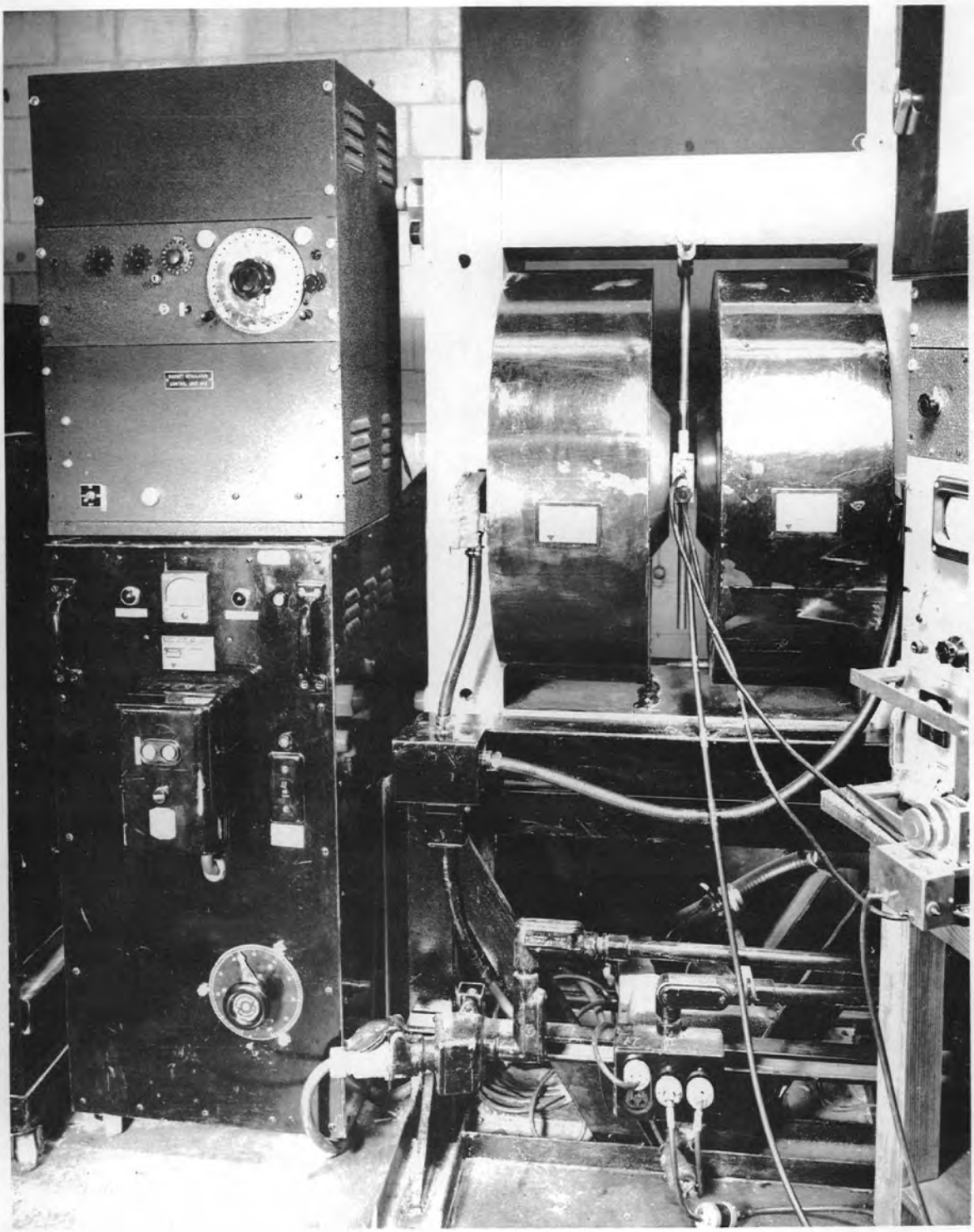

Figure 9. Photograph of electromagnet and power supply

which is insulated from the wire by fish paper and 0.007-inch mica. The entire unit is sealed with insulating compound. For cooling, a water flow of 2 to 3 gallons per minute is required at full magnet power. When assembled each coil weighs approximately 750 lbs.

The magnet is excited by direct current from an a-c power source and rectifier and is capable of supplying 16,500 gauss at its full rated current of 2 amperes and 4KW power. A plot of the magnetic flux characteristics as a function of exciting current is given as Figure 10. Additional interchangeable pole caps have been provided that will give a pole diameter of 12 inches at the 1.75 inch gap. The field strength when using these caps is also indicated in Figure 10.

By using a nuclear resonance detector the homogeneity of the magnetic field has been checked at several locations and at several field strengths. A graph showing the deviations of the field strength over the 8-inch pole caps at a field of 9600 gauss is given in Figure 11. The magnet had been operated for several hours prior to taking the measurements and a uniform hysteresis condition had been established by cycling the field around the ambient value several times. Field homogeneity was determined by photographic records of the resonance from deuterium in D_2O in a 0.5 cm^3 sample.

Power for energizing the magnet is supplied from a 3-phase full-wave rectifier operating from the 460-volt mains. This rectifier is capable of supplying 3800 volts at 2 amperes continuously. A gross filtering of the 360-cycle ripple is performed by an L-C filter section. The direct current output is series regulated by means of a high gain direct coupled regulator amplifier which controls the voltage drop across

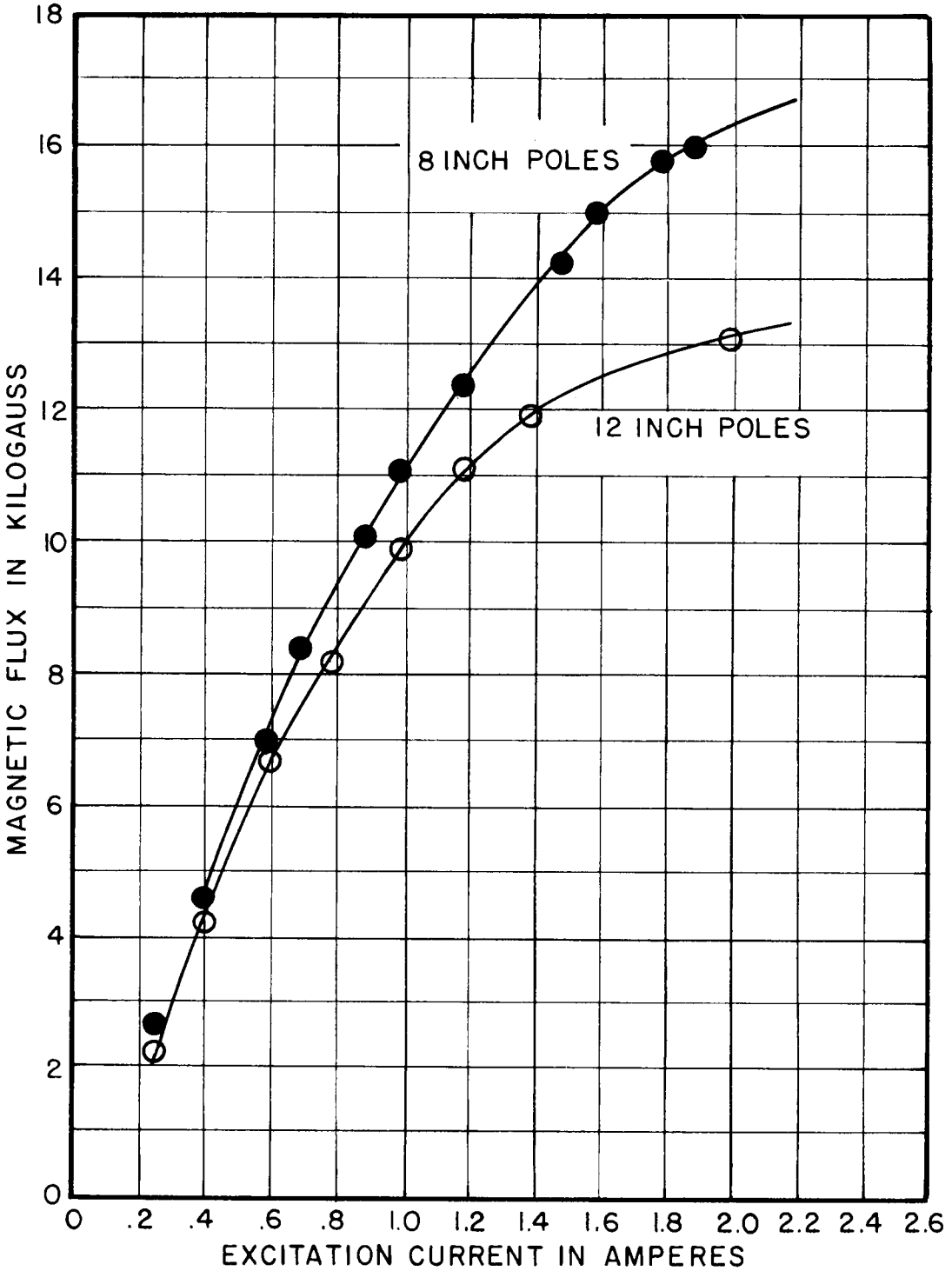

Figure 10. Calibration curve for electromagnet

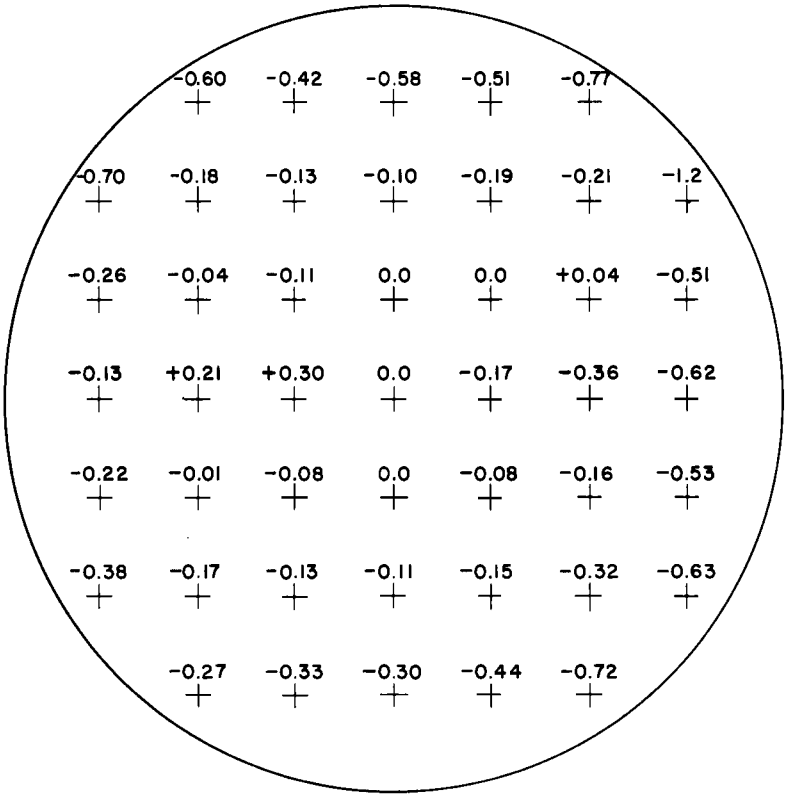

Figure 11. Deviations in the magnetic field strength in gauss for the 8 inch pole caps a field of 9600 gauss

8 parallel connected 304-TL triode tubes. Provision for operating these tubes in the most suitable region for all values of magnetic field is made by controlling the level of the rectified voltage by means of powerstats in the primary supply lines. Schematic wiring diagrams for the power supply and the current regulator are given as Figure 12 and 13 respectively.

The direct coupled current regulator receives its error signal from the magnet current which flows through a precision manganin resistor of about 50 ohms. The temperature of the resistor is held constant for a period of time, long compared with the measurement period, by submerging the resistance winding in an oil bath which is cooled by tap water passing through copper tubing. A photograph of the resistor installed in the series regulator cabinet is given as Figure 14. The voltage drop from this series resistor is balanced against the voltage from a reference standard, and the deviation from balance is used to regulate the current. During search for new resonances and in the slow passage technique it is necessary to vary the magnetic field at a very slow rate. This is done by causing a motor to drive a multi-turn potentiometer connected in the standard battery circuit. Different "scanning" speeds are achieved with the same drive motor by electrical switching of the scanning potentiometer. The wiring diagram for this circuit is given as Figure 15.

By direct measurement the control transconductance for the entire regulator system is in the range 50 to 65 mhos depending upon the supply voltage for the series tubes. The usual operating value corresponds to a system sensitivity of about 63.8 μa/μv. Thus, a change of 1 μv in the

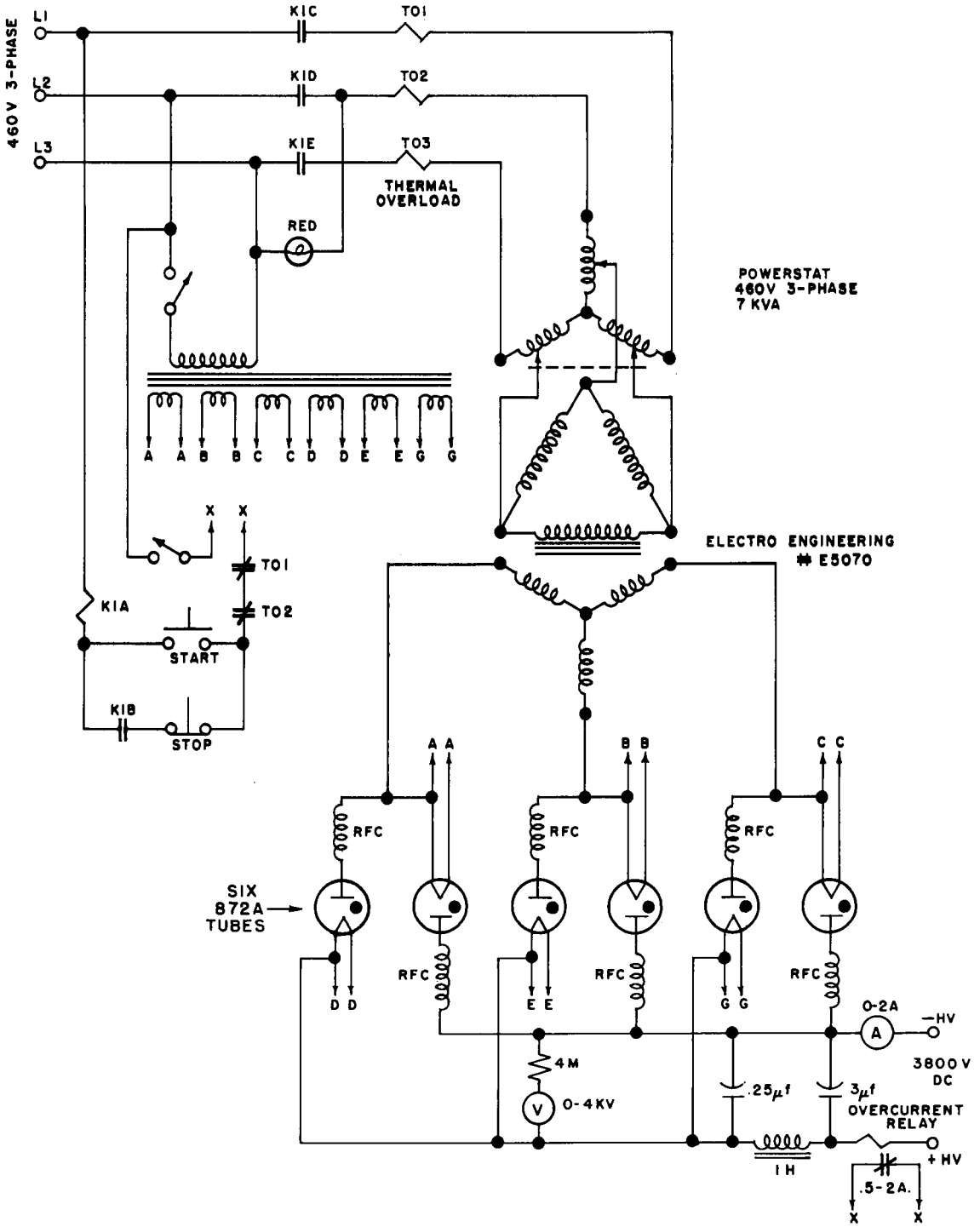

Figure 12. Schematic wiring diagram of high voltage power control and rectifier

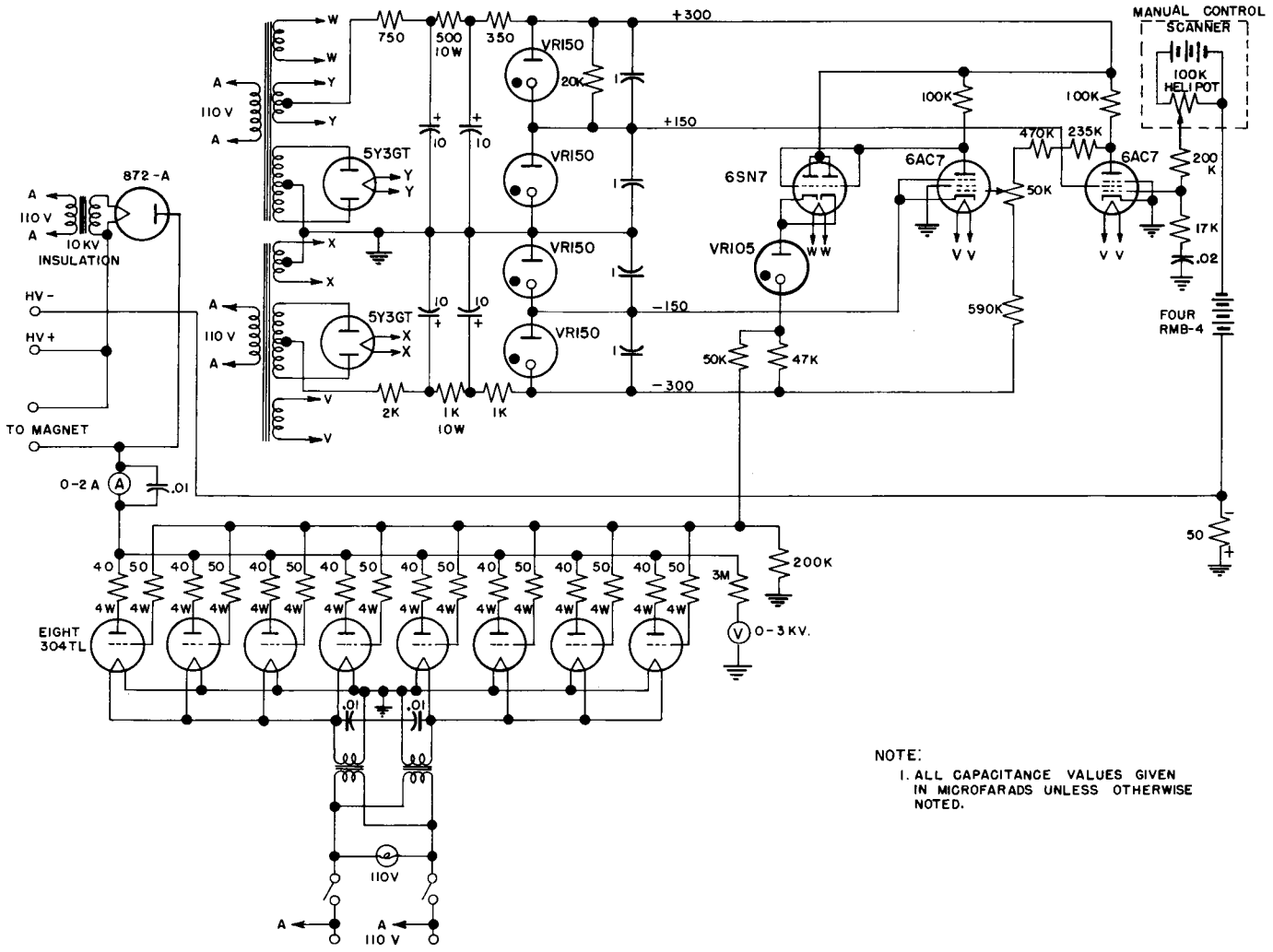

NOTE:
1. ALL CAPACITANCE VALUES GIVEN IN MICROFARADS UNLESS OTHERWISE NOTED.

Figure 13. Schematic wiring diagram of series current regulator and direct coupled magnet control amplifier

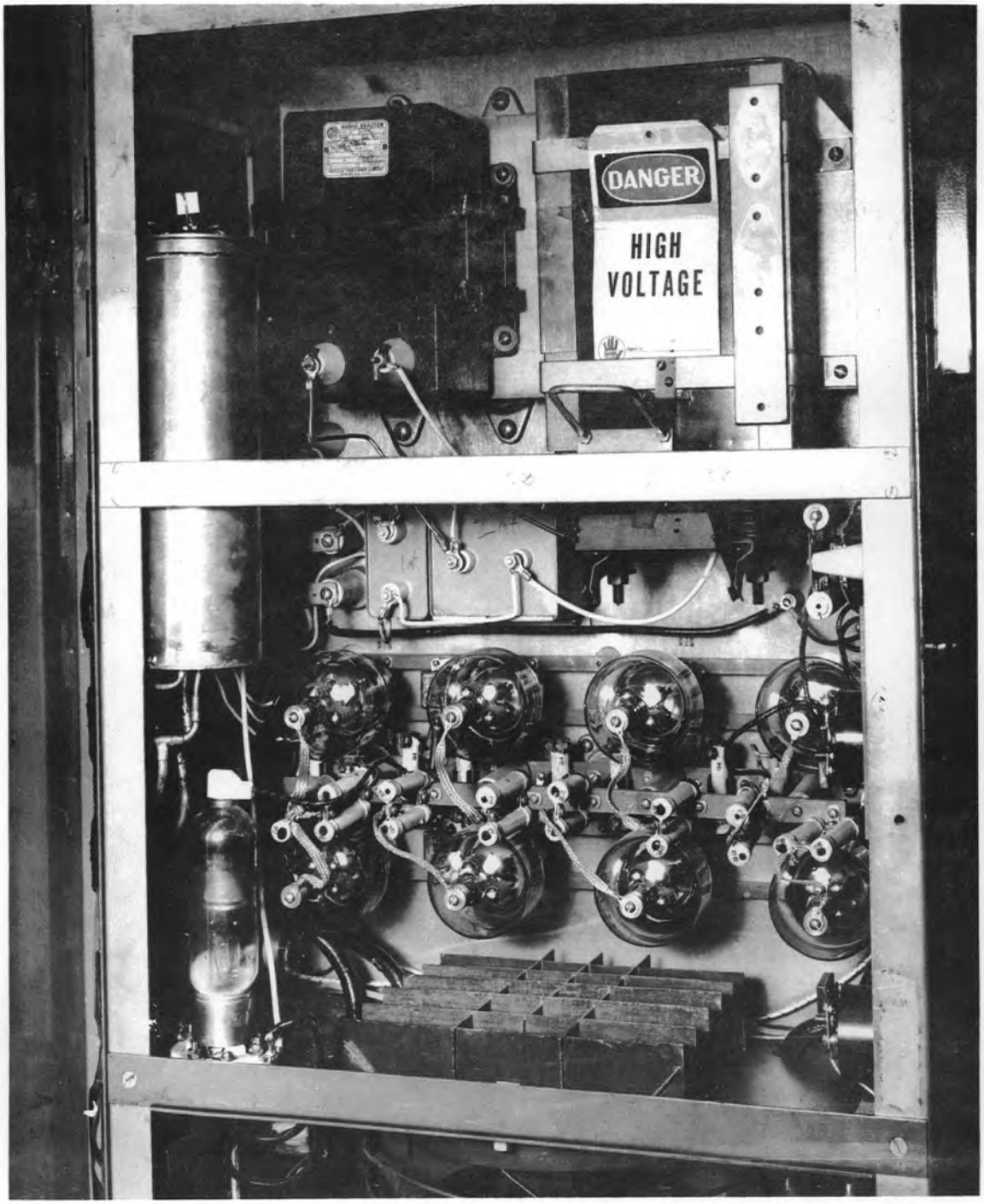

Figure 14. Photograph of precision resistor installed in series current control section of magnet current regulator

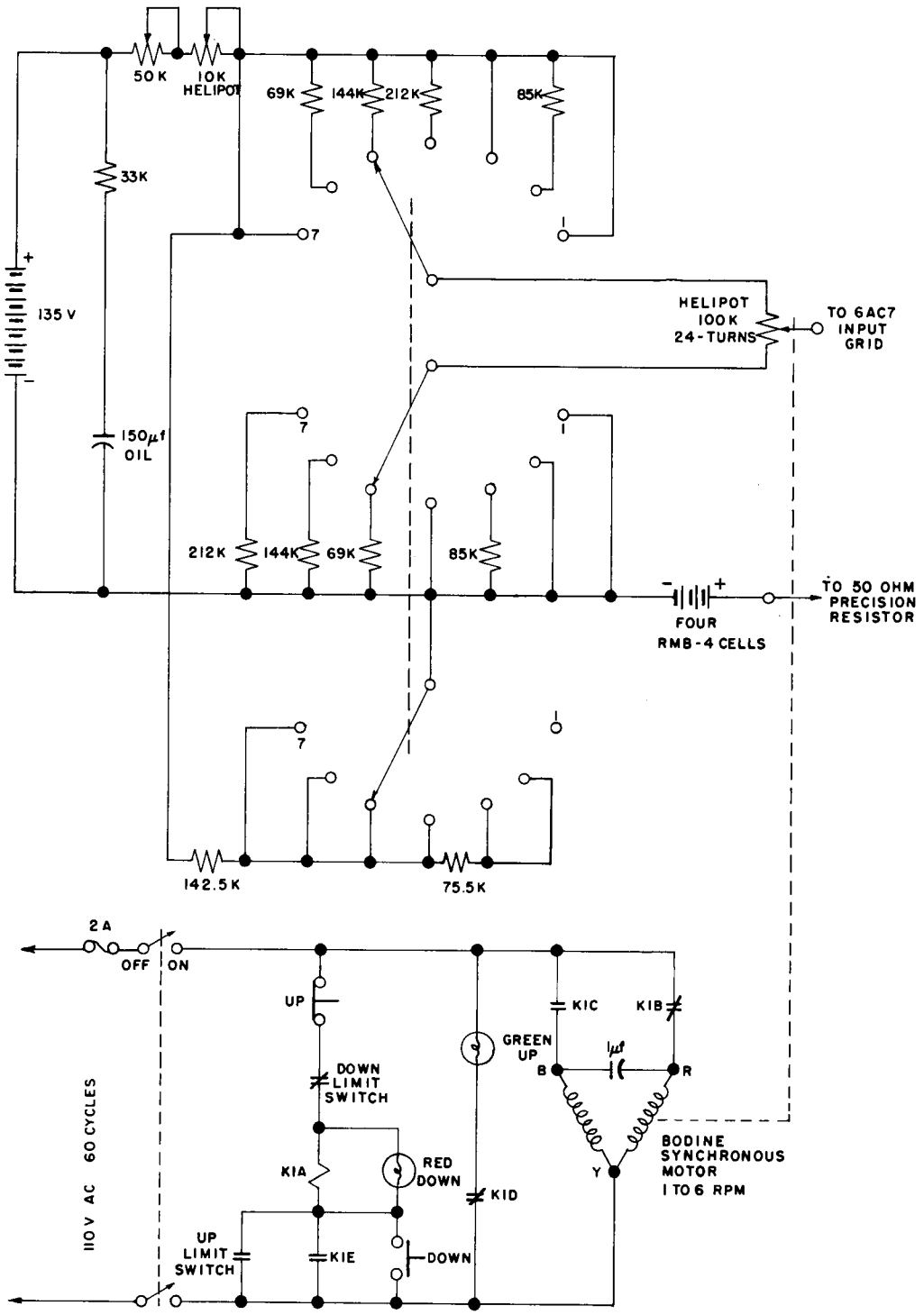

Figure 15. Schematic wiring diagram of control unit for scanning magnetic field

voltage reference will cause a change of 0.638 gauss in the magnetic field in the region 1000 to 10,000 gauss.

The high frequency regulation of the system provides an instantaneous stability of greater than 0.01 gauss, but a slow drift which can amount to as much as 1 gauss per minute is attributed to changes in the circuit resistances, the "standard" reference voltage, and amplifier drift. High frequency response is damped out by an R-C filter at the amplifier input and by the magnet time constant which is about 5 seconds.

In order that the nuclear magnetization be modulated for detection purposes, a small alternating field in the low audio frequency region is applied in the direction of the steady field by means of a pair of Helmholtz coils wound on the spectrometer head case. These will be described in detail in a later section, but are actually part of the magnetic circuit. The modulating coils receive their excitation current from either a Hewlett Packard 200C audio oscillator and a 6L6 output amplifier, or from a sweep generator built into the spectrometer. Modulating fields from zero to about 10 gauss are available.

THE FREQUENCY MEASURING SYSTEM

The fundamental instrument for determining the frequency is a Rauland Army Signal Corps BC-221-AC frequency meter. This frequency meter is factory calibrated at points about 333 kc apart in the region normally used. Using the factory calibration, errors in the order of 1000 cycles are found in certain portions of the spectrum and a further

error is introduced by the rounding off of interpolation data. This error has been greatly reduced by the use of an additional Millen type 90501 secondary frequency standard which has output in 10 kc steps throughout the low megacycle region. The BC-221 is zeroed with the Millen in accordance with its calibration curve at the 10 kc point nearest the resonant value. In this manner practically no deviation is noted from the calibration curve and new interpolation data may be found if desired. Dial calibrations on the BC-221 permit direct frequency interpolation to within 60 cycles for any frequency near 6 mc and to within 30 cycles in the frequency range between 2 and 4 mc. Each of the frequency sources is crystal calibrated with a 1000 kc crystal. When being used they are left running continuously and reach equilibrium temperature after a few hours. Each crystal is brought to zero beat with the 10 or 20 mc signal from the National Bureau of Standards Station WWV. Deviations in frequency between the two crystals does not exceed more than a few cycles per second for periods of several hours and sometimes even days.

For purposes of monitoring the transmitter a National HRO receiver is available. Beat notes between the transmitter and the internal heterodyne oscillator of the BC-221 can be more easily followed on the receiver than with the BC-221 itself. The vertical plates of an oscilloscope can be connected to the HRO second detector output and with 60-cycle line frequency applied to the horizontal sweep it is quite easy to tell by the Lissajous pattern when the transmitter and BC-221 heterodyne oscillator pass through the point where their frequency difference is 30 or 60 cycles.

FREQUENCY MEASURING TECHNIQUES

When using the gyromagnetic ratio of the proton as a means for determining the magnetic field strength our problem changes from that of measuring the magnetic flux to that of determining the frequency of resonance for the proton sample. If the magnetic field is held constant during a ratio measurement, we may determine the gyromagnetic factor of an unknown with respect to that of the proton by measuring the resonant frequency for each and computing their γ ratio, that is, since $\nu = \gamma\psi H$,

$$\nu_x/\nu_p = \gamma_x/\gamma_p \tag{44}$$

We need not know the value of the magnetic field. In the event that the magnetic field fluctuates this relation is no longer true. Once any other nuclide has been measured with sufficient accuracy it may be used as a secondary standard.

For accurate frequency measurements a method must be used where a continuous check can be kept on the accuracy of the frequency meters. This is accomplished in the following manner. The Millen secondary frequency standard is adjusted to within one or two cycles per minute of the 10 mc signal from WWV. It is then decoupled from the receiver and the crystal controlled output of the BC-221 is then also brought to within one or two cycles per minute of the 10 mc signal from WWV. The WWV signal is then removed from the receiver and the Millen and BC-221 are heterodyned together. If the beat note between them is less than two cycles per second they are probably adjusted to the same side of the WWV carrier, but if the beat note is more than two cps one is readjusted

with WWV and the difference is brought to a minimum. Since a difference frequency of 2 cycles per second is not audible through the HRO audio system it is necessary to detect this beat by noting the fluctuation in the AVC voltage which will vary periodically at the difference frequency if both signals are adjusted for approximately the same amplitude at the receiver input.

An alternate technique is to modulate one of the carriers or supply an audible heterodyne by means of a third very weak oscillator. The AVC voltage will fluctuate and alter the intensity of the audible tone at the difference frequency. The 10 kc multivibrator output of the Millen is checked by comparing the output near 1 mc with marker pulses from a Tektronix Model 180 Time Mark Generator by using a Tektronix 513D oscilloscope. During measuring periods the output of the Millen standard is beat continuously with the WWV carrier in a separate receiver and the difference frequency produces an audible fluctuation in the standard frequency tones that WWV transmits. The BC-221 calibration is set of the closest 10 kc point from the resonant frequency before each reading is taken. Over-all calibration checks are made at the beginning and end of each run.

In the event that the resonant frequencies for the two nuclides being measured are far apart, a second BC-221 frequency meter is used. This auxiliary meter is calibrated in the same manner as the others. Once the 10 kc points have been established no further adjustments are required after each reading since the dial is varied by only a very small amount. A quick check is usually made a few times during a run as well as at the beginning and end. Frequently when the resonant

frequencies are far apart three receivers are used, one to heterodyne with the transmitter at each frequency, and one to beat with WWV. In this manner much time can be saved since only the transmitter frequency must be readjusted and there is less opportunity for the magnetic field and frequency meters to drift. Power for all the frequency measuring equipment as well as for the spectrometer itself is obtained through Raytheon voltage stabilizers.

During the period of a "run" certain fluctuations and drifts occur in the magnetic field. In general the regulation of the field is about 1 part in 100,000 but long time drifts are considerably larger than this. These are observed in the data by a continual changing of the resonant frequencies in the same direction. To correct for this drifting, a graphical plotting of the frequencies is made with respect to time and a linear field interpolation is performed. If the frequencies do not indicate a linear or continuous drift no time interpolation is employed.

When the magnetic field is held constant it is necessary to vary the transmitter frequency uniformly across the resonance. This is accomplished by causing the condenser controlling the transmitter frequency to be rotated by a small motor. During a run which usually consists of about 15 different readings, the resonance is always approached from the same frequency direction. On alternate runs this direction is reversed. Measurement of the resonant frequencies is performed alternately, however in this case the resonant frequency is approached by the frequency meter first from the lower side and then from the upper side for each nuclide. This technique tends to lessen

the effects of dial backlash and systematic error. Usually the output of the recording meter is watched and when the center of resonance is reached the frequency meter is brought to zero beat with the transmitter. The scanning speed is slow enough that from 10 to 30 seconds is required to pass through the complete resonance curve. Some error is introduced by the fact that the recorder and lock-in detector have a time constant associated with them that prevents the immediate reproducing of the line center at the moment of attaining this center. Consequently, the frequency that is determined is in slight error, the amount depending upon the signal width, amplitude, and scanning speed. Usually the time constant of the recorder is kept short compared with the time to traverse the signal width, but on extremely weak signals this can not always be achieved because the longer time constant is required to integrate out the noise components. In these cases the error in measuring the frequency may be several hundred cycles. An additional error is introduced by the pen drag, which for an Esterline Angus recording meter is in the order of 3% at full scale. For small amplitudes and relatively large signals having a small amount of high frequency noise the noise component keeps the pen in motion a sufficient amount of the time to reduce the pen drag to a point where it can be neglected.

An additional error that may be quite large is that due to the incomplete balancing of the spectrometer for either the u or v mode, in which case the resulting curve is a mixture of the two modes. The true center of resonance may not be where it would appear to be and errors as large as half of the signal width can be made. Usually they

are much smaller and with careful balancing the line center can be determined to within 10 percent of the line width.

Under conditions where the resonances are quite close together in frequency, direct measurement of the frequencies can be taken from the recorded tape. In such a method a signal from the secondary frequency standard is fed into the spectrometer system and heterodyning with the transmitter causes "pips" to be recorded on the tape at the standard frequencies. Interpolation of the resonant frequency can then be made directly on the chart and is linear for closely spaced resonances. For resonances separated by more than 100 kc the interpolation will be modified by system non-linearities.

THE NUCLEAR INDUCTION SPECTROMETER

Spectrometer is the name given to the remaining nuclear induction equipment. It consists of the radio-frequency transmitter, the "head" unit, the high sensitivity radio-frequency amplifier and detector, the narrow-band high gain audio amplifier, the synchronous detector and recorder circuits, and the circuits for supplying the modulating field, $H_m \cos \omega_m t$. Each is discussed in the following paragraphs. A photograph showing the equipment in operation is included as Figure 16.

The Head Unit

The proper design and construction of the head unit will, for the case of weak signals, determine the success of the experiment; for it is in this unit that a balancing of the radio-frequency fields is

Figure 16. Assembly of nuclear induction equipment—left to right—series magnet current regulator, high voltage rectifier and scanner control, electromagnet, spectrometer and recorders, frequency measuring equipment and a second spectrometer

made and the fundamental signal-to-noise ratio established. The unit must be constructed with great rigidity to prevent vibration in the magnetic field due to the forces created by the currents in the oscillator and modulating field coils which interact with the strong fixed field. The individual components must be precisely machined to give a smooth and continuous adjusting action for precise balancing. An assembly detail drawing of the head unit is included as Figure 17. The head is immersed in the strong magnetic field and no ferro-magnetic materials are permitted to be used, since they would cause impairment of the magnetic field homogeneity in the region of the sample. In this unit it is desirable that all metallic parts except the coil windings themselves be given a silver plate to prevent high r-f losses and a resulting reduction in Q of the tuned circuits. The supports for the transmitting and detecting coils can be made from any insulating material usable in the megacycle r-f range such as Plexiglas, Lucite, polystyrene, or other vinyl plastics.

For certain research purposes it may be desirable that a head be provided that has no inherent residual proton resonance. Each of the above listed materials has an abundance of hydrogen nuclei and gives a large proton signal from the small amount of material contained within the coils. With high sensitivities it is possible to detect the copper isotope resonances due to the copper from which the coils are wound. In order that a proton-free head be available one unit was constructed from the fluorocarbon compound teflon and is discussed here in detail.

The detector coil is wound on the teflon bobbin L in Figure 17. In the frequency range 2-3 mc, for which this particular unit was

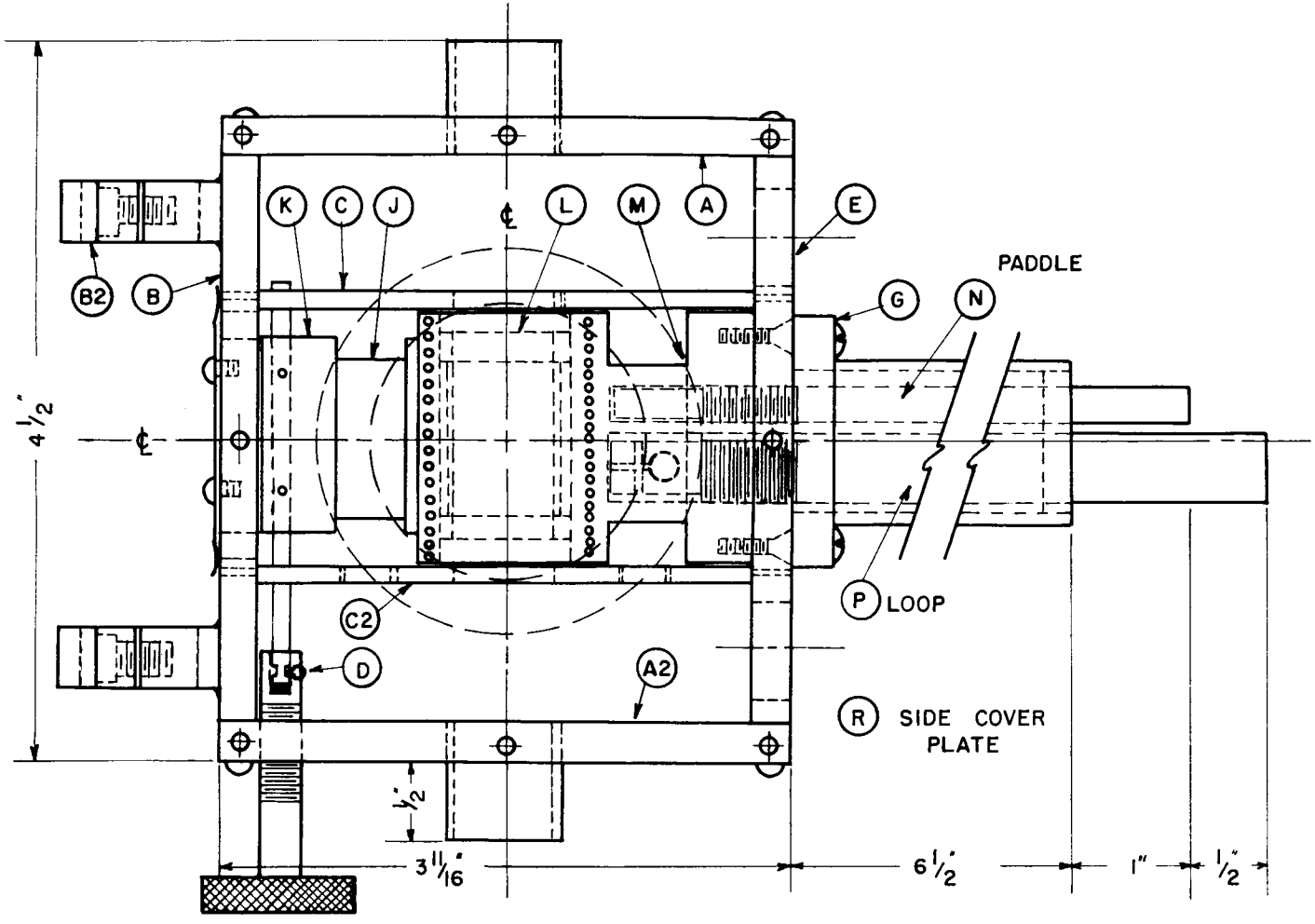

Figure 17. Assembly and detail drawing for nuclear induction head unit

designed, optimum Q can be achieved for a ratio of diameter to length of about 1. The coil is wound with 65 turns of #32 double Formex insulated copper wire with a space factor of 0.6 and to a length of 1 inch. The free air inductance if 60 microhenries. Placing the coil in the shielded silver plated brass box A reduces this inductance by about 50 percent due to the induced eddy currents in the cross braces C and side plates R. This also reduces the free air calculated Q[14] from 140 to less than 100. Insertion of the sample reduces this Q even further. The transmitter coil is wound with half its turns on form M and half on form J. It is wound with about 65 turns of #26 double Formvar and is adjusted through trial and error to have the same in-place inductance as the detector coil in order that the system might track over the usable frequency range. Since the transmitter coil does not determine the frequency of the oscillator, a greatly reduced Q can be utilized. The power that must be dissipated is of the order of a few watts so that a reasonably large wire size is desirable. Coupling between the transmitter and detector field is adjusted by the physical machining of the component M which is held to within a fraction of a degree of the desired 90 degrees.

These coils are mounted in a brass box A, and supported and shielded by brass plates C. One half of the transmitter coil can be translated along the Y-axis by means of a finely machined thread on assembly D. The coil support J is guided by a machined brass insert K which moves in a slot milled in the rear plate B. The whole assembly is enclosed with side plates R on which are wound coils of Helmholtz proportions containing 15 turns each of #16 double cotton covered

magnet wire. These provide a modulating field of about 1.6 gauss per ampere.

Fine balance of the in-phase component of the transmitter field H_1 is made by rotation of the loop control P on its 3/8-40 threads. The paddle control N is similarly rotated by its 1/4-40 threaded shaft. Electrostatic coupling between the transmitter and detector coil is minimized by a Faraday shield formed by grounding non-shorting wires threaded through holes in the coil support M. The entire unit is held firmly in the magnetic field by a support rod passing through mounting brackets B-2 and is given further support by wedging between the pole faces with brass or wooden wedges.

The Radio-Frequency Amplifier and Detector

Excluding the head unit, the radio-frequency amplifier and detector is the most important part of the spectrometer. A schematic diagram of the amplifier appears as Figure 18. The amplifier tube is a 6AK5 or WE 404A. The inductance of the detector coil in the head unit is modified by the variable slug-tuned coil L3 which is resonated by condenser C3 and made to track with the plate network L4,C4 by use of the small padder capacitors. Half of a 6SN7 tube is used to operate a milliammeter to determine when head balancing has been achieved. A small voltage is fed to the grid of the r-f amplifier from the transmitter phase shifter (see Figure 19) to cancel the leakage voltage or to supply quadrature voltage if necessary or desired. In general use, some leakage is desired to cause the 6AL5 diode to operate in the linear

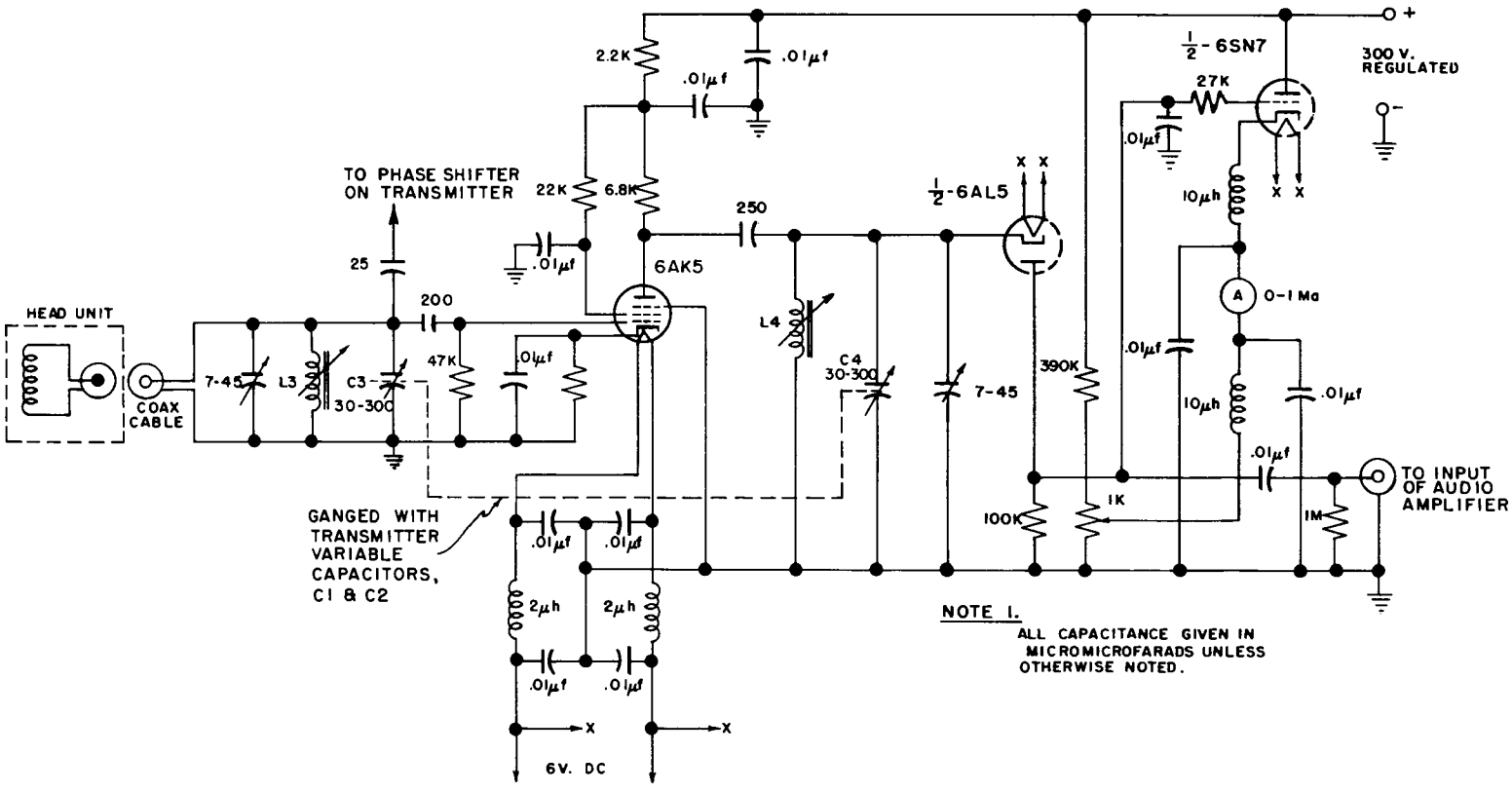

Figure 18. Radio-frequency amplifier and detector

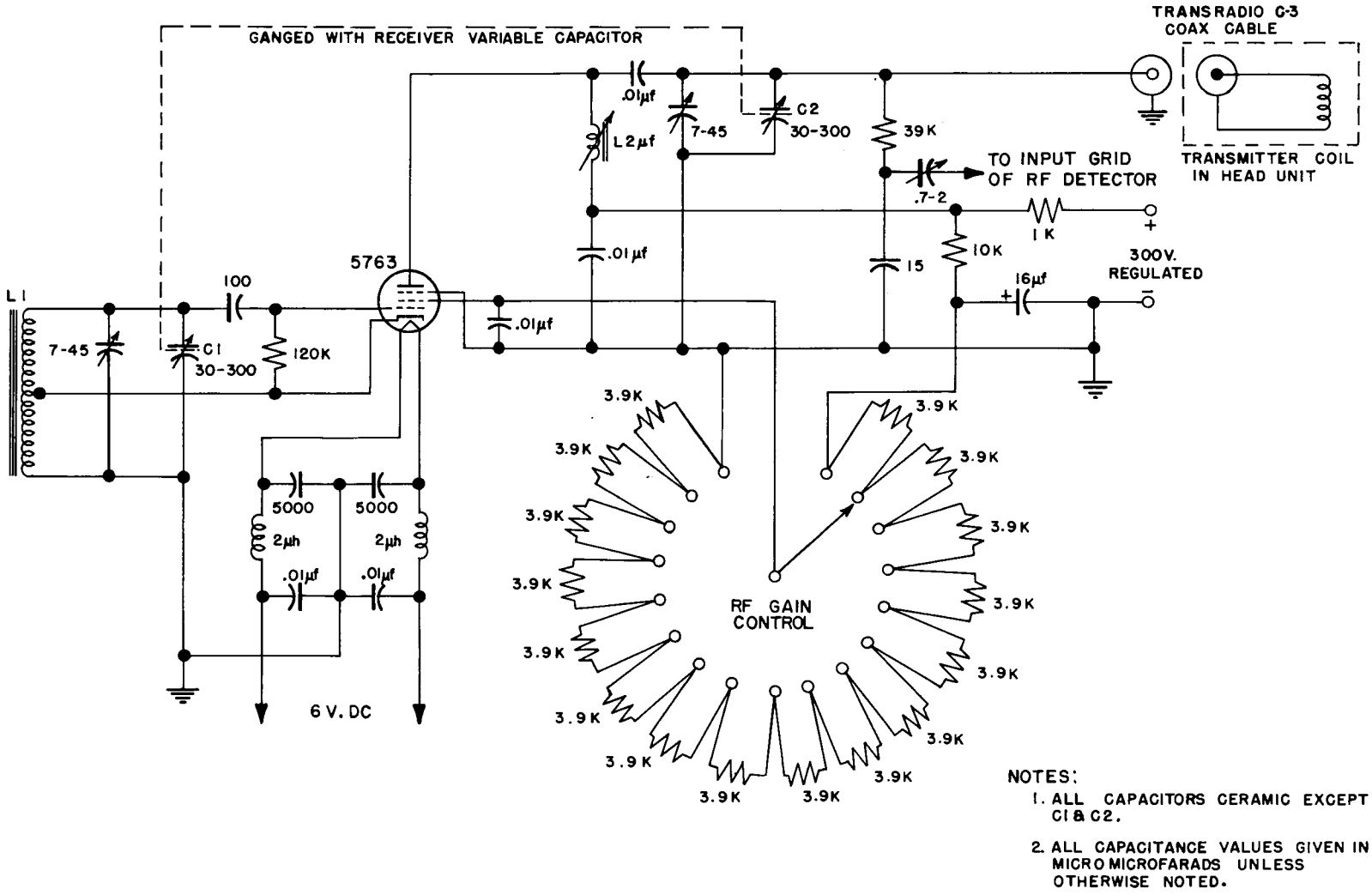

NOTES:

1. ALL CAPACITORS CERAMIC EXCEPT C1 & C2.
2. ALL CAPACITANCE VALUES GIVEN IN MICRO MICROFARADS UNLESS OTHERWISE NOTED.

Figure 19. Schematic diagram of transmitter unit

portion of its operating curve. In this instrument from 0.3 to 0.5 volt of leakage is desirable. The signal due to the resonance has an alternating component at the modulating frequency ω_m which is passed to the input of the high gain audio amplifier.

The Transmitter

The transmitter consists of a single electron-coupled 5763 oscillator which is capable of supplying the transmitter coils with about ten watts of r-f power. Its schematic diagram is Figure 19. The r-f amplitude is controlled by the potential of the 5763 screen. The networks L1,C1 and L2,C2 and the transmitter head coil are adjusted to track with the receiver networks over the tuning range. C1, C2,C3, and C4 are a single shaft variable condenser. When frequency scanning is preferred this tuning condenser is driven by an external motor and a 100:1 reduction worm gear which provides a scanning rate of a few kilocycles per minute. This motor arrangement can be seen in the photograph of Figure 16. The R-C phase shifting network supplies a very small signal to the detector input grid for balancing purposes.

The Amplifier

The audio modulation from the detected resonance is amplified by the high gain amplifier of Figure 20. Low noise 5693 tubes are used in a feedback amplifier. A twin-T feedback network tuned to the modulating frequency is used to reduce the bandwidth of the system when the selector switch is placed in the "narrow" position. A graph showing the

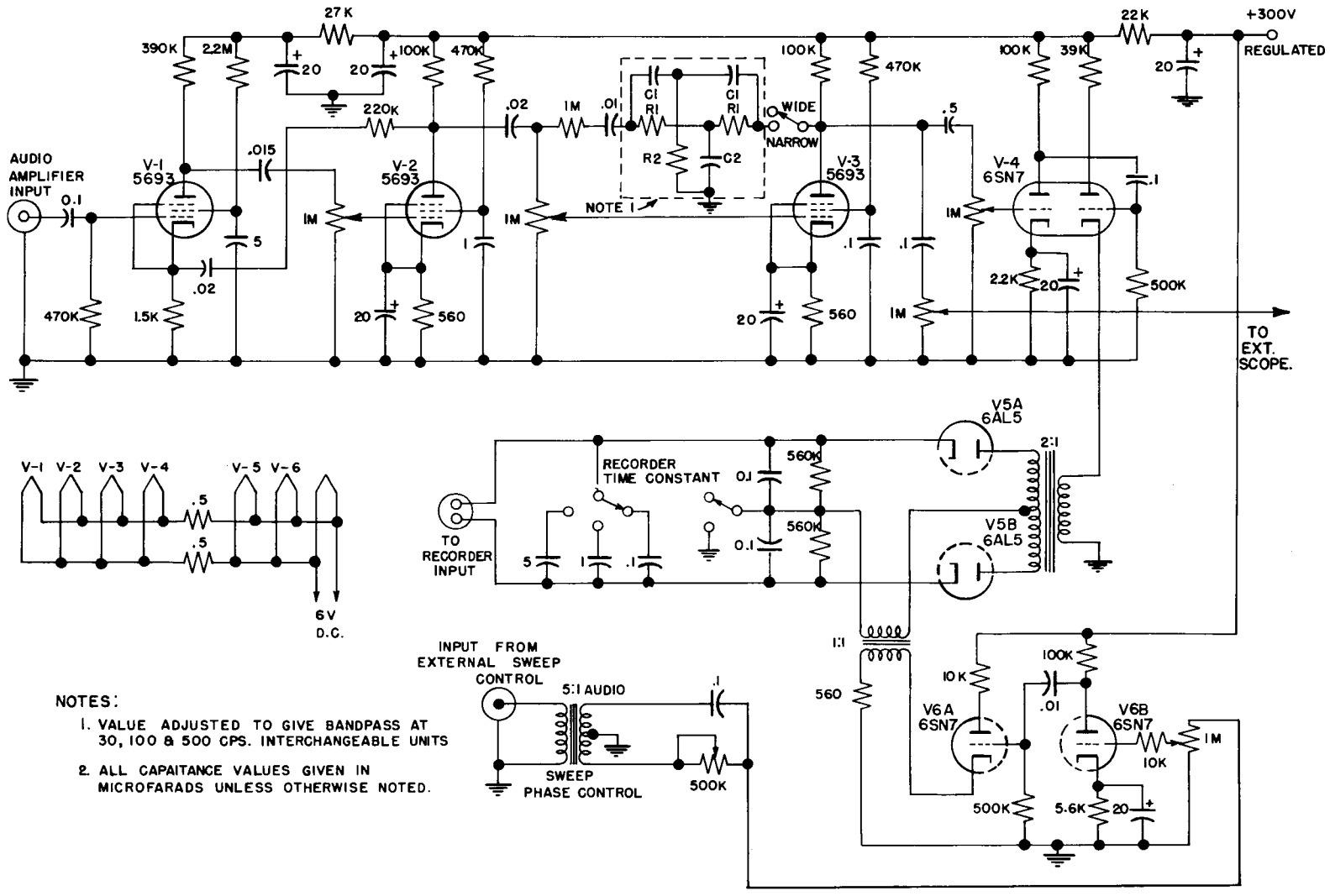

NOTES:

1. VALUE ADJUSTED TO GIVE BANDPASS AT 30, 100 & 500 CPS. INTERCHANGEABLE UNITS
2. ALL CAPAITANCE VALUES GIVEN IN MICROFARADS UNLESS OTHERWISE NOTED.

Figure 20. High gain narrow-band amplifier and phase sensitive detector unit

amplifier gain characteristics with and without a network tuned to 500 cps is given in Figure 21. The signal at the output of the 5693 is then either displayed on an oscilloscope in the form shown previously in Figures 5 and 6 or is coupled by means of a cathode-follower stage to the input of a half-wave phase sensitive detector which receives its synchronizing voltage from the external modulating field voltage source. The phase of the synchronizing voltage can be adjusted to compensate for circuit phase shift.

The output of the phase sensitive detector is direct voltage, the polarity of which is dependent upon the phase relationship of the input and synchronizing voltages. The fluctuations in the d-c level are smoothed out by the selection of a suitable capacitor at the time constant selector switch. The amplitude of this direct voltage varies from about 0.1 volt (due to noise) to 150 volts at system saturation. The d-c signal is applied to the recorder chassis where a vacuum tube voltmeter circuit causes the d-c signal to be recorded by either an Esterline Angus recording milliammeter or a Brown Electronik recorder. The wiring for the recorder chassis is shown in Figure 22.

The Modulating Field

The modulating field is supplied by 15 turns of #16 enameled double cotton covered wire wound into pancake coils which are cemented firmly in place in milled grooves on either side of the brass box surrounding the head coils. For a homogeneous modulating field the coils should have Helmholtz proportions, which for this instrument give a

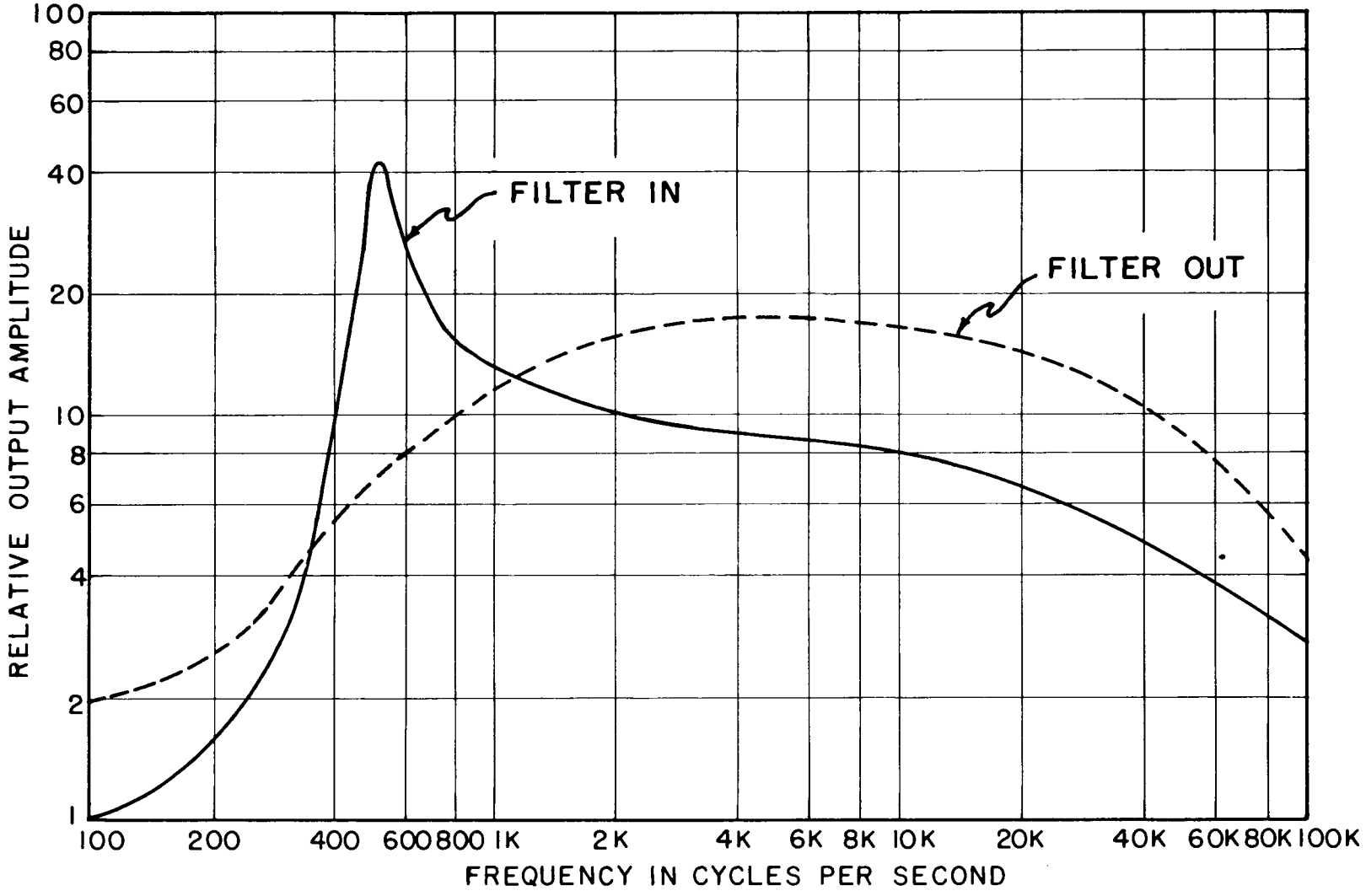

Figure 21. High gain amplifier frequency characteristics

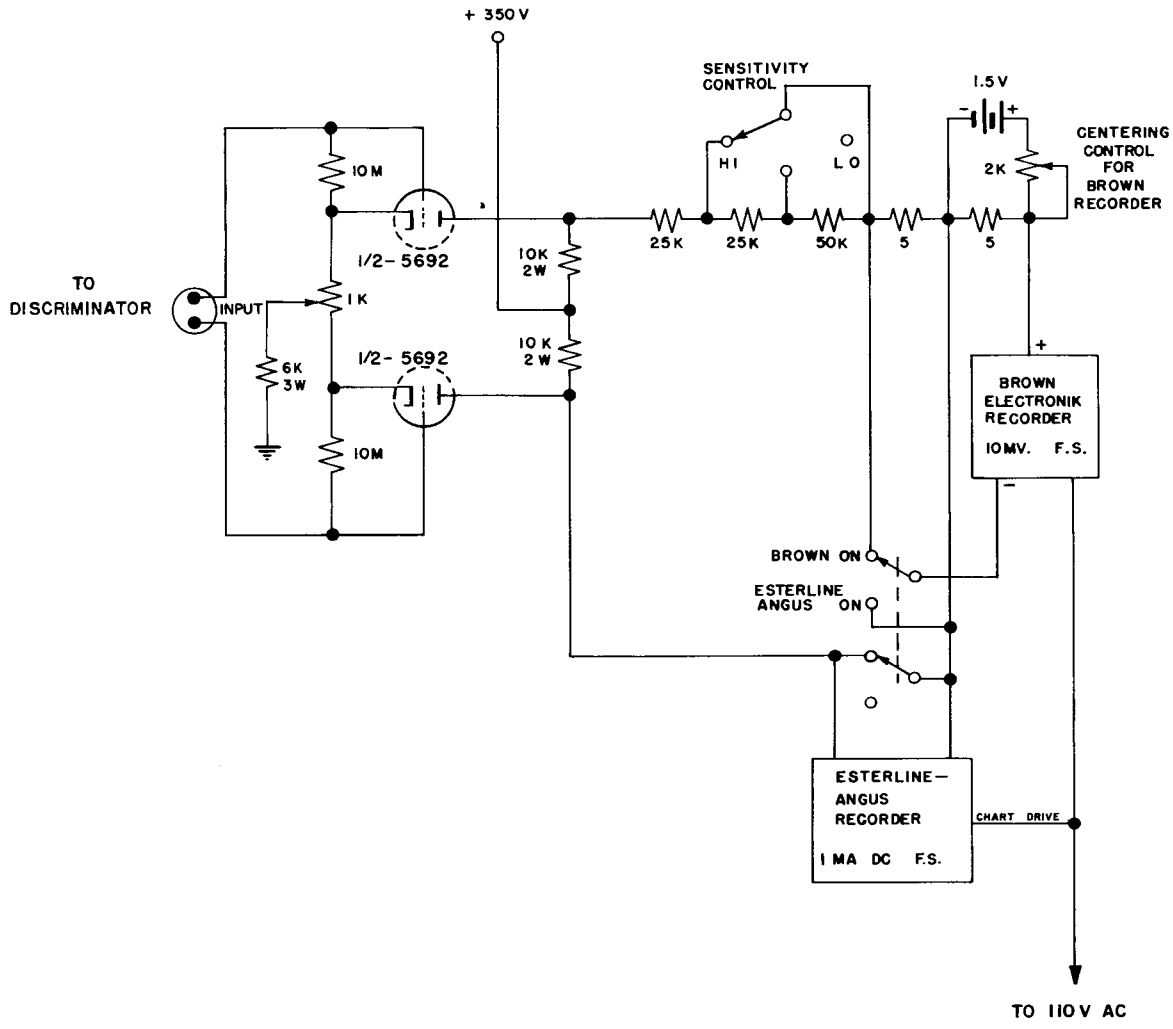

Figure 22. Recorder control panel wiring diagram

resulting average coil diameter of 2 1/2 inches. The coils are driven by a 6L6 amplifier which receives its driving signal from one of three sources as illustrated in Figure 23. These sources are an external oscillator such as the Hewlett Packard HP-200C or its equivalent, a fixed frequency R-C phase shift oscillator shown in Figure 23, or a variable frequency internal oscillator illustrated in Figure 24.

THE RESONANCE MEASUREMENTS

A detailed description of a series of measurements on 17 isotopes of 13 elements will be given in the following paragraphs. The instruments and techniques used are those that have been described in the earlier sections. It has been stated that the characteristics of the sample affect the amplitude and resonance frequency of any nuclide. A detailed description of each experiment will be given and in particular as it concerns the sample conditions. Liquid samples are usually preferable because of the narrow resonances and because the nuclear relaxation times can be easily changed to produce optimum resonance conditions by the addition of paramagnetic ions, commonly referred to as magnetic catalysts. Usually manganese ions are added by dissolving a small amount of the sulphate or chloride into the sample solution. A minimum of catalyst is used in order that excessive magnetic shielding effects are not produced by it. In some instances signals have been observed with satisfactory signal-to-noise ratios without the addition of a catalyst.

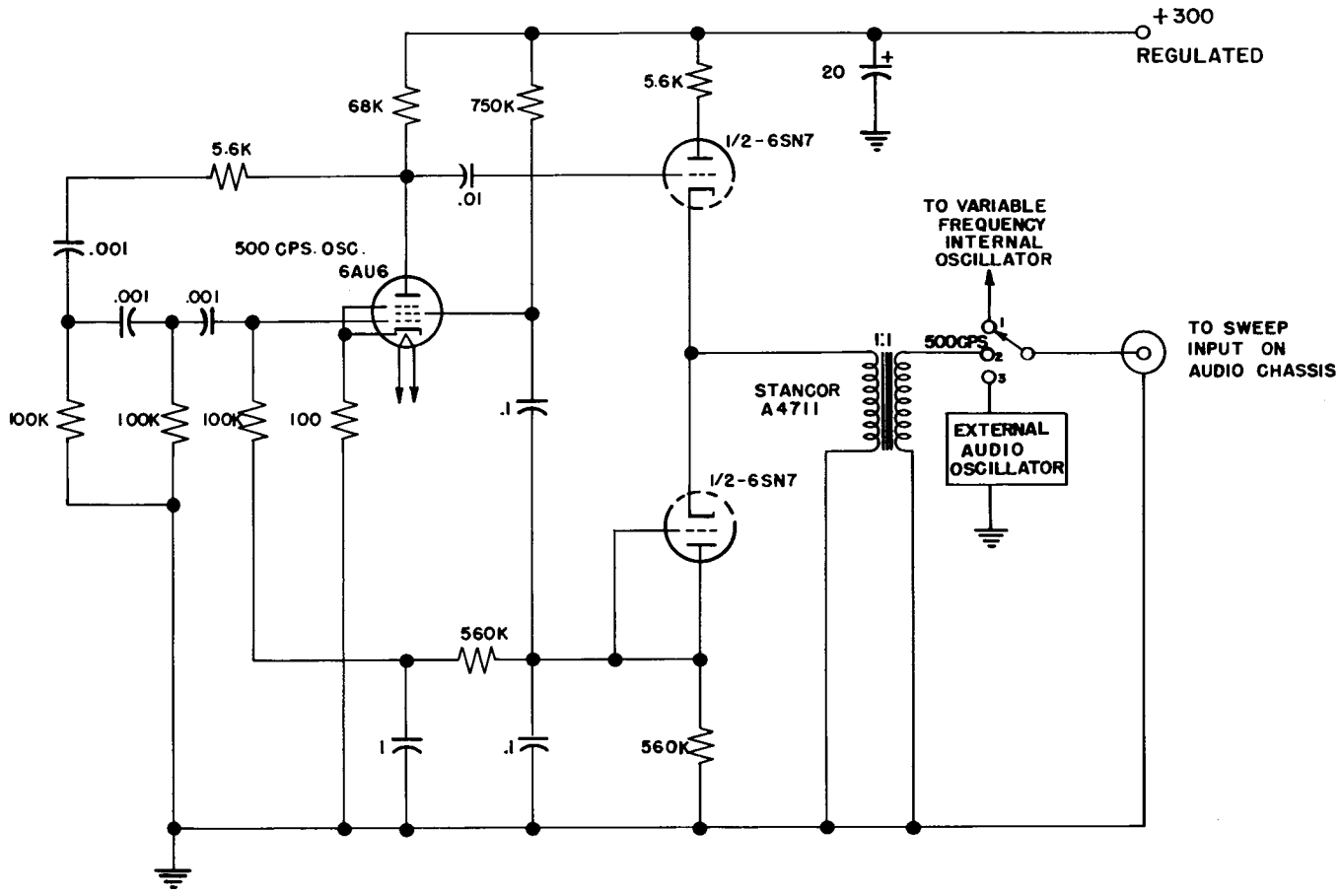

NOTE:

1. ALL CAPACITANCE VALUES GIVEN IN MICROFARADS UNLESS OTHERWISE NOTED.

Figure 23. Sweep modulator selector and 500 cps phase shift oscillator

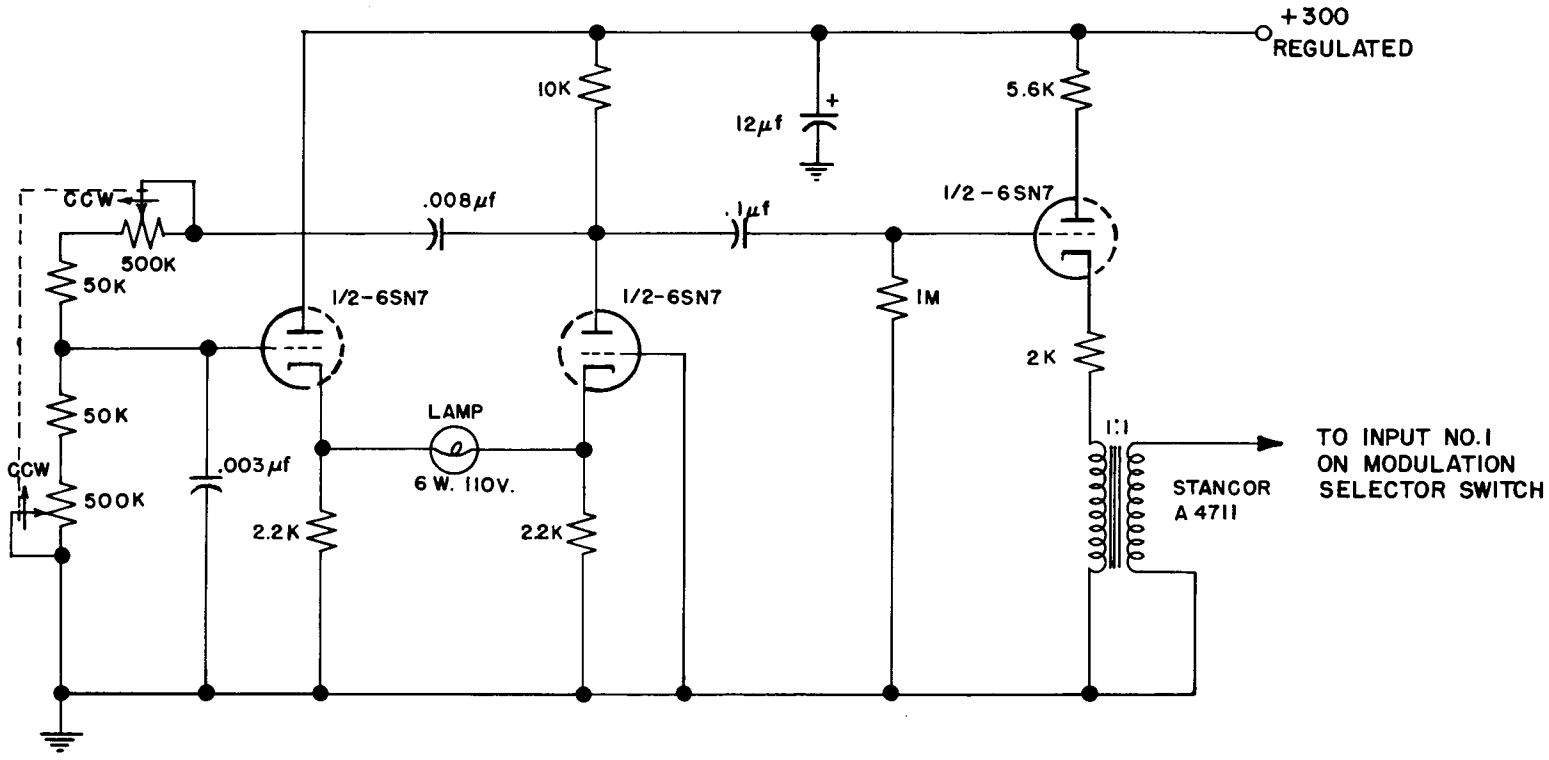

Figure 24. Variable frequency internal modulating field oscillator

Unless otherwise noted the sample volume was approximately 3 cubic centimeters and was positioned into the central portion of the detector coil. A standard 15-mm test tube was the sample holder. The position of the spectrometer head was fixed in the portion of the magnetic field giving the most homogeneous field region; the centerline of the sample fell 1 cm in front of the vertical center line of the pole face and on the horizontal centerline.

Where possible the sample was prepared so as to contain the two nuclei being measured, but where this was not possible because of chemical or other reasons the samples were alternated or otherwise prepared as later described.

Because of the many shielding effects which prevent the measuring of the exact value of the proton and other magnetic moments, any value given for the magnetic moment (μ) of a nuclide would not have the precision possible in the frequency ratio measurements. Therefore a standard value for the nuclear magnetic moment of the proton has been chosen to be 2.79267000 nm (nuclear magnetons) and all values of nuclide moments are compared with this. This value does not include corrections for the diamagnetic effects of the orbital electrons. This value is in essential agreement with the value of Dumond and Cohen[25] as determined by the method of least squares and as discussed on pages 8 and 78 of reference 3. At the present time diamagnetic corrections are known to an accuracy of only 5%.[26] These corrections have therefore not been used in computing the magnetic moments listed herein but are tabulated in reference 2.

The most significant data listed are the nuclide frequency ratios, since for a constant value of magnetic field the ratio of the frequency of resonance for nuclides is proportional to their gyromagnetic ratio. It is this ratio that has been measured and compared with the results of other laboratories. In many instances direct comparisons of results are not possible. In those cases comparisons have been made through the use of frequency ratio products such that ν_x/ν_y is compared with $(\nu_x/\nu_z)\cdot(\nu_z/\nu_y)$. The ratios used in these calculations were chosen either on the basis of the published probable error, or the results of this work were used. In the data tabulation given for each nuclide will be found the degrees of freedom and the standard deviation (σ), which is the square root of the sum of the squares of the deviations from the mean divided by the degrees of freedom. The probable error of the mean is calculated from this value of the standard deviation by use of "t" tables such as given on page 119 of Youden[27] at the 50 percent probability level.

LITHIUM

The resonances of the lithium isotopes 6 and 7 were observed in a saturated aqueous lithium chloride (LiCl) solution containing 0.2 molar manganous sulphate ($MnSO_4$) as a magnetic catalyst and 0.2 cm^3 of deuterium oxide (D_2O). Two experiments of 8 and 9 ratio measurements were performed to measure the lithium to deuterium frequency ratio at fields of 10,000 and 12,000 gauss respectively. The results of these

measurements are given in Table I where the average

$$\nu_{Li\ 6}/\nu_{D\ 2} = 0.958638 \pm 0.000038 \tag{45}$$

Using this ratio, the proton moment, spin I = 1, and Levinthals[28] deuteron to proton ratio of 0.1535062, the magnetic moment is found to be

$$\mu_{Li\ 6} = +\ 0.821921 \text{ nm} \tag{46}$$

The positive sign was indicated by comparison with the deuterium resonance known to have a positive moment.

The lithium 7 to sodium 23 frequency ratio was determined in a single experiment of 9 ratio determinations at a magnetic field near 3250 gauss. The resulting ratio as given in Table I is

$$\nu_{Li\ 7}/\nu_{Na\ 23} = +\ 1.469225 \pm 0.000003 \tag{47}$$

Using the known spin, I = 3/2, a sodium to proton ratio of 0.2645182, and the proton moment, the magnetic moment is

$$\mu_{Li\ 7} = +\ 3.256003 \text{ nm} \tag{48}$$

The positive sign for the moment was confirmed by comparison with the sodium resonance which was known to be positive. These results are compared with other reported values in Table II.

SODIUM

Four experiments of 8 frequency ratio measurements each were performed on a 4 cm^3 aqueous solution of sodium chloride (NaCl) containing 0.2 molar $MnSO_4$ and D_2O. The measurements as tabulated in Table I were made in fields of 6300 and 7000 gauss. The sodium to deuteron frequency ratio was found to be

Table I. Nuclide Frequency Ratio Measurements for Lithium, Sodium, Aluminum, Phosphorus, and Chlorine

Data Table Number	Nuclide Ratio	Frequency Ratio	Standard Deviation ($\times 10^{-6}$)	Degrees of Freedom	Probable Error ($\times 10^{-6}$)
1	Li 6/D 2	0.958636	18	8	5
2	Li 6/D 2	0.958640	114	7	29
Average	Li 6/D 2	0.958638	80	15	38
3	Li 7/Na 23	1.469225	11	7	3
4	Na 23/D 2	1.723274	75	8	18
5	Na 23/D 2	1.723298	68	8	17
6	Na 23/D 2	1.723157	31	7	8
7	Na 23/D 2	1.723128	33	7	9
Average	Na 23/D 2	1.723167	100	30	34
8	Al 27/Na 23	0.985078	32	8	8
9	Al 27/Na 23	0.985022	13	8	3
10	Al 27/Na 23	0.985066	8	8	2
Average	Al 27/Na 23	0.985055	21	24	12
11	P 31/Li 7	1.041619	87	8	21
12	P 31/Li 7	1.041610	21	8	5
Average	P 31/Li 7	1.041611	63	16	30
13	P 31/Na 23	1.530350	81	6	22
14	P 31/Na 23	1.530382	99	5	30
Average	P 31/Na 23	1.530366	84	11	42
15	Cl 35/D 2	0.638302	31	7	8

Table II. Comparisons of Results for Lithium, Sodium, and Aluminum

Comparison Method	Ratio	Probable Error	Reference
	Lithium 6 to Lithium 7		
Direct Measurement	0.378657	0.0000015	29
Direct Measurement	0.37865725	0.00000072	30
(Li 6/D 2)(D 2/H)(H/Na 23)(Na 23/Li 7)	0.378649	0.000010	This Work*
	Lithium 7 to Proton		
Direct Measurement	0.3886341	0.0000002	31
Direct Measurement	0.38862	0.00002	32
Direct Measurement	0.388613	0.000013	33
Direct Measurement	0.388625	0.000038	34
Direct Measurement	0.388637	0.000010	35
(Li 7/Na 23)(Na 23/H)	0.3886368	0.0000008	This Work*
	Sodium 23 to Proton		
Direct Measurement	0.26450	0.00003	34
Direct Measurement	0.26454	0.00007	32
Direct Measurement	0.2645182	0.0000001	31
Direct Measurement	0.264514	- - - -	35
(Na 23/D 2)(D 2/H)	0.264517	0.000005	This Work*
	Aluminum 27 to Proton		
Direct Measurement	0.26056	0.00003	34
Direct Measurement	0.26062	0.00011	32
Direct Measurement	0.2605694	0.0000002	31
Direct Measurement	0.260579	0.000008	35
(Al 27/Na 23)(Na 23/D 2)(D 2/H)	0.260565	0.000006	This Work*

*The precision of these results is impaired by the necessity of using frequency ratio products to obtain the listed value.

$$\nu_{Na\ 23}/\nu_{D\ 2} = 1.723167 \pm 0.000034 \quad (49)$$

Using the spin, I = 3/2, and the deuteron to proton ratio 0.1535062 the nuclear moment without diamagnetic correction becomes

$$\mu_{Na\ 23} = +\ 2.216124\ nm \quad (50)$$

Table II gives a comparison of this result with other published values. The sign was confirmed positive by comparison with the deuterium resonance.

ALUMINUM

A 1.5 cm^3 sample of saturated aqueous NaBr containing 0.2 molar $MnSO_4$ was sealed in a 6-mm glass tube and placed in a 15-mm test tube which was then filled with several cm^3 of saturated aqueous aluminum chloride ($AlCl_3$). Three sets of 9 measurements each were obtained to determine the aluminum to sodium frequency ratio at a field of 7000 gauss. The results of these measurements as listed in Table I indicate the aluminum to sodium ratio to be

$$\nu_{Al\ 27}/\nu_{Na\ 23} = 0.985055 \pm 0.000012 \quad (51)$$

Using a spin value I = 5/2, and the sodium to proton ratio 0.2645182 the magnetic moment is calculated to be

$$\mu_{Al\ 27} = +\ 3.638360\ nm \quad (52)$$

The sign was confirmed positive by comparison with sodium. Table II compares the product of this ratio and the sodium to proton ratio with other published data.

PHOSPHORUS

Four experiments were performed to determine two phosphorus frequency ratios. The phosphorus 31 to lithium 7 ratio was measured in two experiments of 9 ratio determinations each. The sample was a 2 cm^3 sealed glass vial of saturated aqueous LiCl submerged in concentrated phosphoric acid (H_3PO_4) in a 15-mm test tube. The phosphorus 31 to sodium 23 ratio was measured in two experiments and 12 ratio determinations. The sample in this case was H_3PO_4 into which a sealed tube containing approximately 1.5 cm^3 of saturated aqueous sodium bromide (NaBr) with 0.05 molar $MnSO_4$ was placed for a reference source. The results of these measurements are tabulated in Table I where the average ratios are shown to be

$$\nu P\ 31/\nu Li\ 7 = 1.041611 \pm 0.000030 \tag{53}$$

$$\nu P\ 31/\nu Na\ 23 = 1.530366 \pm 0.000040 \tag{54}$$

Using a spin I = 1/2, and the sodium to proton ratio of 0.2645182, the magnetic moment is calculated to be

$$\mu\ P\ 31 = +\ 1.130500\ nm \tag{55}$$

A comparison of this result with other published ratios is given in Table III.

CHLORINE

The resonance of chlorine 35 was observed in a 3 cm^3 saturated aqueous solution of rubidium chloride (RbCl) containing 0.1 cm^3 of D_2O. The chlorine resonance was measured with respect to the deuterium res-

Table III. Comparisons of Results for Phosphorus and Chlorine

Comparison Method	Ratio	Probable Error	Reference
	Phosphorus 31 to Lithium 7		
Direct Measurement	1.04182	0.00005	36
Direct Measurement	1.041611	0.000030	This Work
	Phosphorus 31 to Proton		
Direct Measurement	0.40498	0.0004	37
Direct Measurement	0.40481	0.0004	34
Direct Measurement	0.404804	0.000010	35
(P 31/Na 23)(Na 23/H)	0.404810	0.000012	This Work*
(P 31/Li 7)(Li 7/H)	0.404808	0.000017	This Work*
	Chlorine 35 to Proton		
(Cl 35/Na 23)(Na 23/H)	0.0980066	0.000290	34
Direct Measurement	0.9799	0.00007	37
(Cl 35/Rb 85)(Rb 85/H)	0.0979820	0.0000079	38
(Cl 35/Rb 85)(Rb 85/H)	0.0979796	0.0000020	This Work*
	Chlorine 35 to Deuterium		
Direct Measurement	0.63827	0.00006	29
Direct Measurement	0.638302	0.000008	This Work

*See footnote to Table II pertaining to indirectly determined values.

onance at a field of 10,000 gauss. The results of this experiment of 8 ratio measurements gave the chlorine to deuterium frequency ratio as listed in Table I to be

$$\nu Cl\ 35/\nu D\ 2 = 0.638302 \pm 0.000008 \tag{56}$$

Using a spin, I = 3/2, and Levinthals[28] deuterium to proton ratio, the magnetic moment is calculated to be

$$\mu\ Cl\ 35 = +\ 0.820905\ nm \tag{57}$$

Only one direct chlorine to deuterium measurement has been reported in the literature. Two additional chlorine ratios are reported herein under the paragraphs on rubidium and vanadium measurements. Comparisons with other reported chlorine ratios are made in Table III where all ratios have been converted to that with respect to the proton. The sign of the moment is positive.

VANADIUM

The measurements on vanadium 50 were taken in a series of 7 experiments having 8 ratio measurements each. The sample consisted of 271 mg of vanadium in the form of vanadium oxytrichloride ($VOCl_3$) of which about 10 percent was vanadium 50. Vanadium 50 occurs at an enrichment of about 0.25 percent in nature. This sample was produced in the Calutron electro-magnetic process at Oak Ridge National Laboratory. The $VOCl_3$, a liquid at normal temperatures, was sealed in a small tear drop vial of about 0.5 cm^3 volume and placed in a test tube containing an aqueous solution of 2 mg of RbCl and 0.1 cm^3 D_2O. Measurements were made at fields of 10,600, 11,800, and 14,000 gauss. The results

of these experiments are compiled as given in Table IV. No other measurements have been reported on V 50. The values as listed are

$$\nu V\ 50/\nu Rb\ 85 = 1.032631 \pm 0.000029 \quad (58)$$

$$\nu V\ 50/\nu Cl\ 35 = 1.017583 \pm 0.000011 \quad (59)$$

$$\nu V\ 50/\nu D\ 2 = 0.649518 \pm 0.000008 \quad (60)$$

Using a spin I = 6, an rubidium 85 to proton ratio of 0.09655208[33] and the before listed deuterium to proton ratio the magnetic moment is found to be

$$\mu\ V\ 50 = +\ 3.34128\ nm \quad (61)$$

The sign was determined to be positive by comparison with the deuteron and rubidium resonances.

COPPER

Four experiments were performed to measure the nuclear resonance of copper. Two of these were for the measurement of copper 63 and copper 65 in a sample containing a mixture of Cu_2Cl_2 and $CuCl_2$ and a separate sealed off vial of saturated aqueous NaBr. The remaining two tests measured the copper to sodium frequency ratio in a sample of finely powdered metallic copper and in a NaBr sample. The conduction electrons contribute to the local field in the metal and cause a considerable resonance shift. The finely powdered copper particles have sufficient surface formed oxide to limit eddy currents in the sample and hence permit the copper metal resonance to be detected. However it is a broad resonance in the order of 3 to 4 gauss width at 3 db. points. Measurements were made in a magnetic field near 6600 gauss.

Table IV. Nuclide Frequency Ratio Measurements for Vanadium, Copper, Gallium, and Selenium

Data Table Number	Nuclide Ratio	Frequency Ratio	Standard Deviation ($\times 10^{-6}$)	Degrees of Freedom	Probable Error ($\times 10^{-6}$)
16	V 50/D 2	0.649518	33	7	8
17	V 50/Rb 85	1.032624	67	7	16
18	V 50/Rb 85	1.032525	53	7	13
19	V 50/Rb 85	1.032743	98	7	24
Average	V 50/Rb 85	1.032631	75	21	29
20	V 50/Cl 35	1.017598	17	7	4
21	V 50/Cl 35	1.017621	43	7	11
22	V 50/Cl 35	1.017530	18	7	5
Average	V 50/Cl 35	1.017583	29	21	11
23	Cu 63/Na 23	1.002008	66	7	16
24	Cu 63/Na 23 (metal)	1.004371	59	8	14
25	Cu 65/Na 23	1.073475	42	8	10
26	Cu 65/Na 23 (metal)	1.075960	42	7	11
27	Ga 69/Na 23	0.907381	46	8	11
28	Ga 69/Na 23	0.907316	35	8	8
Average	Ga 69/Na 23	0.907349	41	16	20
29	Ga 71/Na 23	1.152872	33	8	8
30	Se 77/D 2	1.242100	82	8	19
31	Se^{77} in (H_2SeO_3/H_2Se)	1.001498	19	8	5
32	Se^{77} in (H_2SeO_4/H_2SeO_3)	1.001570	120	8	27

The results of these measurements are listed in Table IV and are compared with other published values in Table V. Using the previously stated value for the sodium to proton ratio and a spin, I = 3/2 for the copper isotopes, the magnetic moment is calculated to be

$$\mu \text{ Cu } 63 = + 2.220586 \text{ nm} \tag{62}$$

$$\mu \text{ Cu } 65 = + 2.378967 \text{ nm} \tag{63}$$

The sign is confirmed to be positive by comparison with the sodium resonance. A check in system consistency can be made by comparing the ratio of copper 63 to copper 65 in the Cu_2Cl_2 and in the metal. These calculations give the ratios to be

$$\nu \text{Cu } 65/\nu \text{Cu } 63 = 1.071324 \pm 0.000019 \quad \text{for copper salt} \tag{64}$$

$$\nu \text{Cu } 65/\nu \text{Cu } 63 = 1.071277 \pm 0.000018 \quad \text{for copper metal} \tag{65}$$

A comparison with other laboratory results is given in Table V.

GALLIUM

The nuclear resonances of gallium 69 and gallium 71 were measured with respect to sodium 23 in three experiments of 9 ratio measurements each. The sample consisted of a solution of gallium chloride ($GaCl_3$) made by dissolving gallium metal in hydrochloric acid. A small amount of NaCl was dissolved in the solution to provide the sodium resonance. Measurements were made in magnetic fields of 6100, 6900, and 7200 gauss. The signs of both nuclides were confirmed to be positive by comparison with the sodium resonance. The results of the measurements appear in Table IV and are summarized here.

$$\nu \text{Ga } 69/\nu \text{Na } 23 = 0.907349 \pm 0.000020 \tag{66}$$

Table V. Comparisons of Results for Copper and Gallium

Comparison Method	Ratio	Probable Error	Reference
	Copper 63 to Sodium 23		
Direct Measurement	1.00209	0.00005	40
Direct Measurement	1.0022	0.0002	41
Direct Measurement	1.002008	0.000016	This Work
	Copper 63 to Proton		
Direct Measurement	0.265056	0.000053	34
Direct Measurement	0.26515	0.00005	32
(Cu 63/Na 23)(Na 23/H)	0.265049	0.000005	This Work*
	Copper 65 to Proton		
Direct Measurement	0.28391	0.00006	34
Direct Measurement	0.28404	0.00009	32
(Cu 65/Na 23)(Na 23/H)	0.283954	0.000004	This Work*
	Copper 65 to Copper 63		
Direct Measurement	1.0711	0.0002	41
Direct Measurement	1.07178	0.00005	36
(Cu 65/Na 23)(Na 23/Cu 63)	1.071324	0.000019	This Work*
In metal:(Cu 65/Na 23)(Na 23/Cu 63)	1.071277	0.000018	This Work*
	Gallium 71 to Sodium 23		
Direct Measurement	1.1529	0.0004	43
Direct Measurement	1.152872	0.000008	This Work
	Gallium 71 to Gallium 69		
Direct Measurement	1.27059	0.00008	42
Direct Measurement	1.2701	0.0004	43
(Ga 71/Na 23)(Na 23/Ga 69)	1.27059	0.000023	This Work*

*See footnote to Table II pertaining to indirectly determined values.

$$\nu \text{Ga } 71/\nu \text{Na } 23 = 1.152872 \pm 0.000008 \quad (67)$$

Using the known spin I = 3/2 and the 0.2645182 sodium to proton ratio, the calculated nuclear moments become

$$\mu \text{ Ga } 69 = +\ 2.010809 \text{ nm} \quad (68)$$

$$\mu \text{ Ga } 71 = +\ 2.554922 \text{ nm} \quad (69)$$

A calculated ratio of the nuclides is compared with previously measured and published data in Table V.

SELENIUM

The resonance frequency of selenium 77 was measured relative to that of deuterium in D_2O. The selenium sample was 2 cm^3 of liquid H_2Se which was solidified with liquid nitrogen and sealed in a high pressure boiler gauge tube which held the sample in the liquid condition at room temperature. The deuteron resonance was found in a 1 cm^3 sample of D_2O containing 1 molar $MnSO_4$. Because of the sample size the selenium and deuterium samples were interchanged for each reading but the head unit was not moved during the experiment and both samples were subjected to the same magnetic field area.

A value for the selenium resonance was measured simultaneously at Stanford University[44] but was found to differ from this measured value. To determine the cause for this large difference two additional experiments were performed. In the first of these the D_2O sample was replaced by a sample of H_2SeO_4 and the frequency of the Se 77 resonance was determined in both the H_2Se and the H_2SeO_4. In the second experiment the H_2SeO_4 was replaced by H_2SeO_3 and the Se 77 frequency again

measured. The results of these experiments indicated that a large shift occurs in the selenium resonance in these compounds with the resonance of the H_2Se sample occurring at the lower frequency (field constant) and thus exhibiting the least diamagnetic shielding due to the chemical or compound effects. These measurements were made at a magnetic field near 9100 gauss. The results of these experiments are given in Table IV. A comparison with the results of Dharmatti and Weaver[44] is made through the use of our Se 77 ratio determinations and the sodium to proton, and deuterium to proton ratios, and the results are tabulated in Table VI.

Using our measured Se 77 ratio from H_2Se the magnetic moment for spin, I = 1/2 is calculated to be

$$\mu \text{ Se } 77 = + 0.5324786 \text{ nm} \tag{70}$$

The sign of the moment was found to be positive by comparison with the deuterium resonance.

BROMINE

The resonance frequency for the bromine isotopes 79 and 81 was measured with respect to the sodium 23 resonance in a saturated aqueous solution of sodium bromide (NaBr). Measurements were made in fields near 7200 gauss where 28 ratio determinations were made. The resonances were very narrow and the signal-to-noise ratio was greater than 200 to 1. The results of these measurements are given in Table VII and compared with those reported by others in Table VI. The ratios found were

$$\nu \text{Br } 79/\nu \text{Na } 23 = 0.947140 \pm 0.000009 \tag{71}$$

Table VI. Comparisons of Results for Selenium, Bromine, and Rubidium

Comparison Method	Ratio	Probable Error	Reference
Selenium 77 to Proton in H_2SeO_3			
Direct Measurement	0.190964	0.000053	44
$H_2Se^{77}O_3/H_2Se^{77}$)(H_2Se/D 2)(D 2/H)	0.190956	0.000003	This Work*
Bromine 79 to Proton			
Direct Measurement	0.25059	0.00005	32
(Br 79/Na 23)(Na 23/H)	0.250536	0.000003	This Work*
Bromine 81 to Sodium 23			
Direct Measurement	1.0209	0.0003	45
Direct Measurement	1.020965	0.000014	This Work
Bromine 81 to Bromine 79			
Direct Measurement	1.0778	0.0003	45
Direct Measurement	1.07775	0.00005	36
Direct Measurement	1.077897	0.000012	This Work
Rubidium 85 to Proton			
Direct Measurement	0.09655208	0.00000001	39
Direct Measurement	0.09661	0.00004	37
(Rb 85/D 2)(D 2/H)	0.0965531	0.000010	This Work*
(Rb 85/Cl 35)(Cl 35/D 2)(D 2/H)	0.0965558	0.000022	This Work*
Rubidium 87 to Proton			
Direct Measurement	0.327228	0.000014	46
Direct Measurement	0.32718	0.00007	34
Direct Measurement	0.32718	0.00016	32
Direct Measurement	0.32721338	0.00000055	39
(Rb 87/Al 27)(Al 27/Na 23)(Na 23/H)	0.327085	0.000012	36
(Rb 87/Na 23)(Na 23/H)	0.3272198	0.000026	This Work*
Rubidium 87 to Rubidium 85			
Direct Measurement	2.033380	0.000028	47
(Rb 87/H)(H/Rb 85)	2.0333899	0.000004	39
(Rb 87/H)(H/Rb 85)	2.033351	0.000016	This Work*

*See footnote to Table II pertaining to indirectly determined values.

ν Br 81/ν Na 23 = 1.020965 ± 0.000014 (72)

The magnetic moments have been calculated using the known spin I = 3/2 and the sodium to proton ratio and are found to be

μ Br 79 = + 2.098991 nm (73)

u Br 81 = + 2.262597 nm (74)

The sign of the moment is confirmed to be positive by comparison with the sodium resonance.

RUBIDIUM

The nuclear resonances of rubidium 85 and 87 were measured with respect to the resonance of chlorine 35 and deuterium in a saturated aqueous sample of rubidium chloride (RbCl) containing a small amount of D_2O. Table VII lists the results of four experiments of 32 ratio measurements on Rb 87. These results are compared with those reported from other laboratories in Table VI. Using the spin I = 5/2 for Rb 87, and I = 3/2 for rubidium 85 and the previously used values for the deuteron to proton, chlorine to deuteron, and sodium to proton ratios the magnetic moments have been calculated to be

μ Rb 85 = + 1.348217 nm (75)

μ Rb 87 = + 2.741451 nm (76)

The sign of both isotopes was confirmed to be positive by comparison with the known resonances of sodium and deuterium.

Table VII. Nuclide Frequency Ratio Measurements for Bromine, Rubidium, Cesium, and Thallium

Data Table Number	Nuclide Ratio	Frequency Ratio	Standard Deviation ($\times 10^{-6}$)	Degrees of Freedom	Probable Error ($\times 10^{-6}$)
33	Br 79/Na 23	0.947140	37	8	9
34	Br 81/Na 23	1.020967	44	8	9
35	Br 81/Na 23	1.020963	22	9	5
Average	Br 81/Na 23	1.020965	34	17	14
36	Br 81/Br 79	1.077897	56	9	12
37	Rb 85/Cl 35	0.985429	76	6	20
38	Rb 85/Cl 35	0.985419	38	7	9
39	Rb 85/Cl 35	0.985445	13	7	31
Average	Rb 85/Cl 35	0.985431	46	20	18
40	Rb 85/D 2	0.628985	20	8	5
41	Rb 87/Na 23	1.237041	34	8	8
42	Cs 133/D 2	0.854481	28	8	7
43	Cs 133/D 2	0.854503	50	5	14
Average	Cs 133/D 2	0.854496	38	13	18
44	Tl 205/Tl 203	1.009827	75	8	17
45	Tl 205/Tl 203	1.009822	48	8	11
46	Tl 205/Tl 203	1.009800	34	9	8
Average	Tl 205/Tl 203	1.009816	55	25	22

CESIUM

The nuclear magnetic resonance frequency of cesium 133 was measured with respect to the resonance frequency of deuterium in a sample of aqueous cesium nitrate ($CsNO_3$) having a 0.3 molar D_2O concentration. The ratio was determined in 15 measurements during two experiments at fields of 11,750 and 12,250 gauss. The results of this test tabulated in Table VII gives the cesium to deuterium ratio to be

$$\nu \text{ Cs } 133/\nu \text{ D } 2 = 0.854496 \pm 0.000018 \tag{77}$$

The sign of the nuclear moment is confirmed to be positive, and the nuclear moment without diamagnetic correction is calculated with the use of the deuterium to proton ratio and I = 7/2 to be

$$\mu \text{ Cs } 133 = + 2.56421 \text{ nm} \tag{78}$$

A comparison with other published values is given in Table VIII.

THALLIUM

The ratio of the nuclear moments of the thallium isotopes Tl 203 and Tl 205 was measured in a 6 cm^3 sample of 1.1 molar thallous acetate ($Tl(C_2H_3O_2)$) in a field of 2900 gauss. Because of the large frequency difference between the thallium resonance and a convenient reference nuclide the thallium was not measured with respect to any other element. The ratios obtained for the two thallium isotopes are listed in Table VII and compared with other reported values in Table VIII.

Table VIII. Comparisons of Results for Cesium and Thallium

Comparison Method	Ratio	Probable Error	Reference
	Cesium 133 to Deuterium		
Direct Measurement	0.85449	0.00004	36
(Cs 133/H)(H/D 2)	0.85293	0.00091	37
(Cs 133/Li 7)(Li 7/H)(H/D 2)	0.85428	0.00030	34
Direct Measurement	0.854496	0.000018	This Work
	Thallium 205 to Thallium 203		
Direct Measurement	1.00986	0.00005	49
Direct Measurement	1.00983	0.00005	36
Direct Measurement	1.0098	0.0002	50
Direct Measurement	1.009838	0.000001	48
Direct Measurement	1.009816	0.000022	This Work

PRECISION OF EXPERIMENTS

Using the nuclear spectrometer herein described it is possible to measure frequencies to within about 60 cycles. In the region used this amounts to about 1 part in 100,000. Additional accuracy in the determination of frequencies could be achieved through use of an oscilloscope and Lissajous figures and a calibrated audio oscillator. This was not justified with the present equipment because it is not possible to determine the center of the resonance curve to any better than the 60 cycle limit. This minimum error is determined in general by the ability to read the dial of the frequency meter once a line center has been established. It is possible to observe the point of zero-beat between the oscillator and the frequency meter to within two cps, but backlash in the dial, and vernier accuracy does not permit reading and interpolating to better than the 60-cycle limit. The limitation in the measuring of the center of the line width varies with each nuclide and is dependent upon the signal-to-noise ratio present as well as upon the degree of balance of the r-f modes, and the field inhomogeneity. In general, for a symmetrical curve, it is possible to estimate the line center to within 5 to 10 percent of the line width. During the nuclide frequency measurements the magnetic field was held constant and the frequency was varied to detect the various resonances. In such a system, any drifting of the magnetic field causes a direct error to be recorded in the measured ratio. In fact, for most of the cases listed the magnetic field error was by far the largest error present. When new bat-

teries were installed as the voltage reference source the long period drift of the magnetic field was constant at a rate of about -0.05 gauss per minute at fields near 10,000 gauss. Under extreme conditions of drift the rate became as high as -0.5 gauss per minute. New batteries were stabilized for a period of 24 hours under normal current load before using them as a standard voltage reference source. Most of the field instability is due to drift in the high gain direct coupled amplifiers used in the magnet regulator. The high frequency response and stability of the current regulator was such as to give a maximum field fluctuation due to noise and momentary impulses in the order of 1 part in 10^5 to 1 part in 10^6 for periods of 0.05 seconds and introduced negligible error. A curve of the magnetic field strength versus time gives a straight line indicating a linear field drift at a uniform rate for periods as long as 8 hours. At least four different sets of voltage standard cells were used over the period of several months in which the measurements were made and each time the same linear changes were observed so that it was felt safe to apply a linear time interpolation to the frequencies measured for each experiment. Occasionally an unaccounted for shift would occur in the absolute field strength and the drift would continue on from that point with the same linear rate. Because of these shifts the frequency time interpolations were made only from adjacent points and no data was retained where an obvious jump had occurred. A sample of the method used in computing the listed values is given as Appendix IV.

The overall accuracy of any measurement should lie between 1 part in 10^4 and 1 part in 10^5 depending upon signal conditions. The precision

of the experiments were, in general, much better than this. As an example consider the sequence of measurements on vanadium and rubidium. The measured value for the νV 50/νCl 35 ratio was found to be νV 50/νCl 35 = 1.017583, and by using the individually measured ratios for νV 50/νRb 85 and νCl 35/νRb 85 the calculated νV 50/νCl 35 ratio is 1.017586. Here the deviation is 3 parts in 10^6 and is well within the calculated probable error of 0.000011. A similar case, but one in which the confidence limits are much less due to a smaller number of measurements, is the ratio of νP 31/νLi 7. Here the directly measured value was 1.041611 and the calculated value using the individually measured νP 31/νNa 23 and νNa 23/νLi 7 ratios is 1.041614. The difference is again 3 parts in 10^6 but the probable error of the directly measured value is 0.000030.

No limits of error have been given for the values of the nuclear moment since the value obtained will vary with compound and chemical shielding. Neglecting the diamagnetic correction, which was not applied to these values, the absolute value should be accurate to 0.1 percent for all nuclides and to 0.01 percent for most of the nuclides.

SUGGESTED IMPROVEMENTS

Operation of this equipment has brought forth a number of suggested improvements which should be considered in the construction of future units.

The magnet stability could be improved and the drift lessened appreciably by replacing the direct coupled amplifier with a high gain

feedback amplifier and chopper system. Short period stabilities of the order of 1 part in 10^7 should be obtainable for periods of a few seconds and the long term drift would be virtually eliminated except for changes caused by the standard cell voltage and precision series current measuring resistor.

Increased spectrometer sensitivity through the use of more rigidly constructed head units and the use of a cascade coupled r-f input stage would permit the use of smaller sample sizes and a resultingly smaller field volume which would tend to decrease the line width through increased field homogeneity.

Use of a high speed pen recorder such as the Brush d-c amplifier and 100 cycle recording pen would permit faster and more uniform resonance responses and better center frequency determinations. High resolution equipment would permit direct observation of the resonance and beating frequency on the spectrometer oscilloscope for some of the stronger nuclide resonances.

SUMMARY

The magnetic moments of nuclei in matter will in general result in a nuclear paramagnetic polarization upon reaching an equilibrium in a constant magnetic field. A radio-frequency field at right angles to the constant field causes a precession of this total polarization about the steady field. When the radio-frequency field is adjusted to a frequency corresponding with the Larmor frequency for the nuclei there results a component of the nuclear polarization at right angles to both the constant and the radio-frequency field which is used to induce a voltage in a suitably placed pick-up coil mounted with its axis perpendicular to both of the applied fields. The instrument used to detect this is based upon the "nuclear induction" equipment of Bloch, Hansen, and Packard[12] and is called a nuclear spectrometer. The design, development, and construction of a new improved instrument and its associated magnet and equipment have been discussed in detail. The spectrometer was then successfully used to measure the resonance frequency ratios for 17 isotopes of 13 elements in a fixed magnetic field with a precision greater than that heretofore available. Twelve of these frequency ratios have not been previously measured and the remaining are in agreement with other published values. The design and construction of this spectrometer now makes feasible continued search for the resonances of elements such as rhodium 103, tungsten 183, uranium 235 and the rare earths which all have gyromagnetic factors near 0.2 or less.

REFERENCES

REFERENCES

1. "Resonance Absorption by Nuclear Magnetic Moments in a Solid," E. M. Purcell, H. C. Torrey, R. V. Pound. The Physical Review, volume 69, January 1946, pages 37-38.

2. "Nuclear Induction," F. Bloch, W. W. Hansen, M. E. Packard. The Physical Review, volume 69, March 1946, page 127.

3. A Table of Nuclear Moment Data, ORNL-1469 (report), H. E. Walchli. Office of Technical Services, Department of Commerce, Washington, D. C., 1953, pages 6-78. A listing of measured moments as of June 1953.

4. Ibid., pages 79-102.

5. "Nuclear Magnetic Resonance Multiplets in Liquids," H. S. Gutowsky, D. W. McCall, C. P. Slichter. The Journal of Chemical Physics, volume 21, February 1953, pages 279-292.

6. "Relaxation Effects in Nuclear Magnetic Resonance Absorption," N. Bloembergen, E. M. Purcell, R. V. Pound. The Physical Review, volume 73, April 1, 1948, pages 679-712.

7. "Nuclear Induction," F. Bloch. The Physical Review, volume 70, October 1 and 15, 1946, pages 460-473.

8. "Anamalous Results in an Attempt to Determine the Spin of Si 29," R. H. Sands, G. E. Pake. The Physical Review, volume 89, February 15, 1953, page 896.

9. "The Spin and Magnetic Moment of Ca 43," C. D. Jeffries. The Physical Review, volume 90, June 15, 1953, page 1130.

10. "The Molecular Beam Resonance Method for Measuring Nuclear Magnetic Moments," I. I. Rabi, S. Millman, P. Kusch. The Physical Review, volume 55, March 15, 1939, page 526-534.

11. "Fundamentals of Nuclear Magnetic Resonance Absorption," G. E. Pake. American Journal of Physics, volume 18, October 1950, page 451.

12. "The Nuclear Induction Experiment," F. Bloch, W. W. Hansen, M. Packard. The Physical Review, volume 70, October 1 and 15, 1946, pages 474-485.

13. Principles of Electricity and Electro-magnetism (book), Harnwell. McGraw Hill Book Co., Inc., New York, N. Y., 1949, page 389.

14. Radiotron Designers Handbook (book), Langford-Smith, Editors. Radio Corporation of America, Harrison, N. J., 1952, pages 463-475.

15. "On the Magnetic Moment of Si 29, S 33, Zn 67, As 75, Se 77, Te 123, and Te 125," H. E. Weaver, Jr. Unpublished Ph.D. thesis, Department of Physics, Stanford University, June 1952.

16. "The Dependence of a Nuclear Magnetic Resonance Frequency upon Chemical Compound," W. G. Proctor and F. C. Yu. The Physical Review, volume 77, March 1, 1950, page 717.

17. "Dependence of the F 19 Nuclear Resonance Position on Chemical Compound," W. C. Dickinson. The Physical Review, volume 77, March 1, 1950, page 736.

18. "Magnetic Shielding Effects in Compounds of Vanadium," H. E. Walchli, H. W. Morgan. The Physical Review, volume 87, August 1, 1952, pages 541-542.

19. "Nuclear Magnetic Resonance Measurements of Selenium," H. E. Walchli. The Physical Review, volume 90, April 15, 1953, pages 331-332.

20. "Spin Echoes," E. L. Hahn. The Physical Review, volume 80, November 15, 1950, pages 580-594.

21. "Transient Nutations in Nuclear Magnetic Resonance," H. C. Torrey. The Physical Review, volume 76, October 15, 1949, pages 1059-1068.

22. "The Time Average Magnetic Field at the Nucleus in Nuclear Magnetic Resonance Experiments," W. C. Dickinson. The Physical Review, volume 81, March 1, 1951, pages 717-731.

23. "Measurement of the Proton Moment in Absolute Units," Thomas, Driscoll, Hipple. The Physical Review, volume 78, June 15, 1950, pages 787-790.

24. "A Direct Determination of the Magnetic Moment of the Protons in Units of the Nuclear Magneton," C. D. Jeffries. The Physical Review, volume 81, March 15, 1951, pages 1040-1055.

25. "Least Squares Adjustment of the Atomic Constants, 1952," Jesse W. M. Dumond, E. Richard Cohen. Review of Modern Physics, volume 25, July 1953, pages 691-708.

26. "Hartree Computation of the Internal Diamagnetic Field for Atoms," W. C. Dickinson. The Physical Review, volume 80, November 15, 1950, page 567.

27. Statistical Methods for Chemists (book), W. J. Youden. John Wiley and Sons, Inc., New York, N. Y., 1951.

28. "Relative Nuclear Moments of H^1 and H^2, E. C. Levinthal. The Physical Review, volume 78, May 1, 1950, pages 204-213.

29. "An Improved RF Spectrometer; g-factor Ratios Li 7/ Li 6 and Cl 35/ Cl 37," G. D. Watkins, R. V. Pound. The Physical Review, volume 82, April 15, 1951, page 343.

30. MIT Research Laboratory of Electronics, Quarterly Progress Report, N. I. Adams, T. F. Wimett, F. Bitter, April 15, 1951.

31. "Nuclear Resonance Absorption Applied to Precise Measurement of Nuclear Magnetic Moments," Gunnar Lindström. Arkiv For Fysik, volume 1, Number 4, 1951, pages 1-80.

32. "Determination of Gyromagnetic Ratios I.," J. R. Zimmerman, D. Williams. The Physical Review, volume 76, August 1, 1949, pages 350-357.

33. "The Nuclear Magnetic Moments of D 2 , Li 7, and F 19 Studied by the Magnetic Resonance Absorption Method," K. Siegbahn, Gunnar Lindström. Arkiv For Fysik, volume 1, Number 6, 1950, pages 193-212. Also see Nature, volume 167, Feb. 5, 1949, page 211.

34. "Gyromagnetic Ratio Determinations," F. Bitter. The Physical Review, volume 75, April 15, 1949, page 1326a.

35. "The Gryomagnetic Ratios of Li 7, Na 23, Al 27, and P 31," T. Kanda, Y. Masuda, R. Kusaka, Y. Yamagato, J. Itoh. The Physical Review, volume 85, March 1, 1952, page 938.

36. "Nuclear Gyromagnetic Ratios III.," R. E. Sheriff, Dudley Williams, The Physical Review, volume 82, June 1, 1951, pages 651-655.

37. "Nuclear Gyromagnetic Ratios II.," W. H. Chambers, Dudley Williams. The Physical Review, volume 76, September 1, 1949, pages 638-640.

38. "Nuclear Gyromagnetic Ratios IV.," Yu Ting, Dudley Williams. The Physical Review, volume 89, February 1, 1953, pages 595-596.

39. "Nuclear Magnetic Moment of Rb 85, Rb 87, and I 127," E. Yasaitis, B. Smaller. The Physical Review, volume 82, June 1, 1951, page 750.

40. "Chemical Application of Nuclear Magnetic Resonance," Shizuo Fujiwara, Shoichi Hayashi. Reports of the University of Electro-Communication, volume 4, December 1952, pages 101-106.

41. "The Magnetic Moments of Cu 63 and Cu 65," R. V. Pound. The Physical Review, volume 73, March 1, 1948, pages 523-524.

42. "On the Hyperfine Structure of Gallium," G. E. Becker, P. Kusch. The Physical Review, volume 73, March 15, 1948, pages 584-591.

43. "On the Nuclear Moments of I 127, Ga 69, Ga 71, and P 31," R. V. Pound. The Physical Review, volume 73, May 1, 1948, pages 1112-1113.

44. "Magnetic Moment of Se 77," S. S. Dharmatti, H. E. Weaver, Jr. The Physical Review, volume 86, April 15, 1952, page 259.

45. "The Nuclear Magnetic Moments of Bromine," R. V. Pound. The Physical Review, volume 72, December 15, 1947, page 1273.

46. MIT Research Laboratory of Electronics, Quarterly Progress Report, N. I. Adams. October 1949.

47. MIT Research Laboratory of Electonics, Magnet Research Laboratory Quarterly Progress Report, F. Bitter, N. I. Adams, J. Brossel, H. H. Plotkin, P. L. Sagalyn, T. F. Wimett. December 1, 1950, pages 44-46.

48. "Nuclear Magnetic Resonance in Thallium Compounds," H. S. Gutowsky, B. R. McGarvey. The Physical Review, volume 91, July 1, 1953, pages 81-86.

49. MIT Research Laboratory of Electronics, Report No. 74, H. L. Poss. July 28, 1948.

50. "The Magnetic Moment of Tl 203," W. G. Proctor. The Physical Review, volume 75, February 1, 1949, pages 522-523.

APPENDIX I.

Appendix I. Relaxation Times

In order to observe the effects of energy transitions that take place under resonance conditions it is necessary that an uneven distribution of nuclei occur among the various Zeeman energy levels. Since the transition probabilities for absorption and induced emission are equal, there would otherwise be no net absorption of energy. The magnetic field at the nucleus is composed of the applied field plus perturbing fields due to interactions between the nuclei and the atoms. These interactions permit energy to be transferred to the surroundings and a thermal equilibrium can be established. The energy difference between nuclear Zeeman levels in the fields used is much less than the equilibrium thermal energy (kT) where T is the lattice temperature. The distribution of population between the various magnetic energy states is governed by the Boltzmann factor

$$\frac{N_{m1}}{N_{m2}} = \frac{e^{-\frac{m_1 \gamma \hbar H}{kT}}}{e^{-\frac{m_2 \gamma \hbar H}{kT}}} = e^{-\frac{\Delta m_i \gamma \hbar H}{kT}} \tag{79}$$

where N_{m1} and N_{m2} are the number of nuclei in states m_1 and m_2, and where the magnetic quantum numbers m_i are given values $I \geq m_i \geq -I$. The distribution ratio is given for small values of $[\Delta m_i \gamma \hbar H/kT]$ by the approximate expression (when $\Delta m_i = -1$)

$$\frac{N_{m1}\ \text{(upper state)}}{N_{m2}\ \text{(lower state)}} = 1 - \frac{\gamma \hbar H}{kT} \tag{80}$$

From this we can easily see that a sample in the earths very small field would have almost equal distributions between the energy levels. Should

the same sample be subjected to a stronger field the energy distributions would become more unequally divided in the amount given by Equation 80. This equilibrium distribution is also a function of the Boltzmann thermal energy kT. Applying energy to the system in the form of a resonating oscillatory field in an amount $h\nu$ redistributes the alignment of the nuclei in the applied steady magnetic field and changes the volume susceptibility of the sample, since the nuclear magnetic susceptibility of a gross nuclear sample is determined by the equilibrium alignment of the nuclear magnetic polarization in the magnetic field which is a direct function of the number of nuclear particles aligned in their specified quantized energy states in the magnetic field. The energy $h\nu$ that is supplied is very much less than the average energy kT. The new nuclear alignment represents a state of higher stored energy than before and one says that the "spin temperature" has been raised. The coupling of this nuclear energy to the atom is loose, being through the spin-lattice force fields; however, it is this coupling that permits a new equilibrium to be reached after a time T_1 called the "spin-lattice" relaxation time.

As an example of this spin temperature phenomenon consider a sample first subjected to the earths magnetic field where the energy distributions are about equal in the various energy states. Then subject this sample to a suddenly applied strong magnetic field of many oersteds. The spin temperature at the first moment (T_{start}) must be higher than the room temperature T because of the sudden application of the strong field since the original population distribution is instantaneously unchanged. After a certain period of time however,

transitions take place, the spins are reoriented, and the spin temperature has cooled to the room temperature T. The time required for T_{start} to approach T is called the spin-lattice relaxation time T_1, or the thermal relaxation time. It is the time required for all but 1/e of the equilibrium excess to reach the lower energy state. Bloch[2] describes this as the time for the Z component of $\bar{\mu}_n$ to attain alignment in the field, and terms it the longitudinal relaxation time.

One might also expect spin-spin interactions to occur between like nuclei precessing with equal rotational frequencies ω_o thereby tending to induce transitions between the Zeeman energy levels in each other. These interactions are termed spin-spin collisions and do not affect the total spin system energy but do limit the lifetime of a spin state and contribute to the frequency breadth of the resonance state. The magnitude of the frequency spread $\delta\omega_o$ due to the local field H_{loc} caused by spin-spin interactions is

$$\delta\omega_o \approx g \frac{\mu_o}{\hbar} H_{loc} \approx \gamma H_{loc} \tag{81}$$

Thus one can say that if two nuclei are precessing in-phase at a time t = 0 they will have lost their phase relationship within a time of the order of $1/\delta\omega_o$. For protons this is of the order of 10^{-4} seconds. This phase memory time is called the spin-spin or transverse relaxation time and is denoted by

$$T_2 = \frac{1}{\delta\omega_o} \quad . \tag{82}$$

T_2 is usually found to be less than T_1.

APPENDIX II.

Appendix II. The Nuclear Complex Susceptibilities

The solutions for the particular case of slow passage in nuclear resonance have been given. The particular solution for M_y, the component of the polarization vector along the Y-axis, Equation 31, has been repeated here

$$M_y = \tfrac{1}{2}\chi_o \omega_o T_2 \left[\frac{2H_1 \cos\omega t - 2H_1 T_2 \Delta\omega \sin\omega t}{1 + (T_2\Delta\omega)^2 + (\gamma H_1)^2 T_1 T_2} \right] \tag{31}$$

If one now expresses the oscillating field H_1 as given in Equation 7 in terms of a complex number

$$\underset{\sim}{H} = 2H_1 \, e^{i(\omega t + \pi/2)} \tag{83}$$

and the magnetization, Equation 9, as the complex expression

$$\underset{\sim}{M} = \underset{\sim}{\chi} \, \underset{\sim}{H} \tag{84}$$

where a complex susceptibility is introduced such that

$$\underset{\sim}{\chi} = \chi' - i\chi''$$

a second equation expressing M_y can be written where

$$M_y = \chi''(2H_1 \cos\omega t) - \chi'(2H_1 \sin\omega t) \tag{85}$$

Upon comparing Equations 31 and 84 the expressions for the components of the susceptibility can be written as

$$\chi' = \tfrac{1}{2}T_2 \chi_o \gamma H_o \frac{(T_2 \Delta\omega)}{1 + (T_2\Delta\omega)^2 + (\gamma H_1)^2 T_1 T_2} \tag{86}$$

and

$$\chi'' = \tfrac{1}{2}T_2 \chi_o \gamma H_o \frac{1}{1 + (T_2\Delta\omega)^2 + (\gamma H_1)^2 T_1 T_2} \tag{87}$$

Upon consideration of the phase relationships one can see that it is the χ'' component that is in-phase with the field H_1.

The power absorbed by the nuclear sample per unit volume is

$$A = \frac{\omega}{2\pi} \int_{t=0}^{t=2\pi/\omega} \bar{H} \cdot d\bar{M} \tag{88}$$

and if $\bar{M}$ and $d\bar{M}/dt$ are colinear with the field $2H_1$, upon substituting Equations 82 and 84 and integrating, the power absorbed is found to be

$$A = 2H_1^2 \omega \chi'' \tag{89}$$

and it is seen that the χ'' component is the portion of the complex susceptibility that corresponds to absorption. This absorbed power is small and is in the order of 10^{-9} watts for a 1 cm^3 sample of water at room temperature.

It is easily seen that for a given set of field conditions the optimum value for χ'' occurs for $\Delta\omega = 0$ when χ'' becomes

$$\chi'' = \tfrac{1}{2} T_2 \gamma \chi_o H_o \frac{1}{1 + (\gamma H_1)^2 T_1 T_2} \tag{90}$$

The component χ' is out-of-phase with the rotating field and gives the dispersion which will asymptotically approach the same maximum value as χ'' for $\Delta\omega = \left[1 + (\gamma H_1)\, T_1 T_2\right]^{\frac{1}{2}}$ when $(\gamma H_1)^2 T_1 T_2 \gg 1$.

APPENDIX III.

Appendix III. Sample Calculations

These calculations are those performed for determining the reported values for the Phosphorus 31 to Sodium 23 ratio.

Data Taken from Table XXI.	Deviations ($\times 10^{-6}$)	Deviations Squared ($\times 10^{-12}$)
1.530428	78	6084
1.530377	27	729
1.530178	172	25584
1.530355	5	25
1.530351	1	1
1.530370	20	400
1.530397	47	2209
Average 1.530350		39032

$\sigma = (39032 \times 10^{-12}/6)^{\frac{1}{2}} = 0.000086$

P.E. $= 0.6745\ \sigma\ n^{-\frac{1}{2}} = 0.000022$

Data Taken from Table XXII.	Deviations ($\times 10^{-6}$)	Deviations Squared ($\times 10^{-12}$)
1.530516	134	17956
1.530332	50	2500
1.530254	128	16384
1.530387	5	25
1.530423	41	1681
1.530235	147	21609
Average 1.530382		60155

$\sigma = (60155 \times 10^{-12}/5)^{\frac{1}{2}} = 0.000110$

P.E. $= 0.6745\ \sigma\ n^{-\frac{1}{2}} = 0.000030$

Table XXI average	1.530350
Table XXII average	1.530382
Set average	1.530366

σ average $= \left[(39032 + 60155) \times 10^{-12}/12\right]^{\frac{1}{2}} = 0.000091$

P.E. average $= 0.6745\ \sigma\ n^{-\frac{1}{2}} = \left[(0.6745)(91 \times 10^{-6})/2\right]^{\frac{1}{2}} = 0.000042$